

1 **Role of Topography in Tropical Cyclogenesis over the Indian Ocean**

2 Caitlin M. Fine, Richard H. Johnson*, Paul E. Ciesielski, and Richard K. Taft

3 *Department of Atmospheric Science, Colorado State University, Fort Collins, Colorado*

4 **Corresponding author address:* Richard H. Johnson, Department of Atmospheric Science, 1371

5 Campus Delivery, Colorado State University, Fort Collins, CO 80523.

6 E-mail: johnson@atmos.colostate.edu

ABSTRACT

7 The role of Sumatra and adjacent topographic features in tropical cyclone
8 (TC) genesis over the Indian Ocean (IO) is investigated. Sumatra, as well as
9 adjacent Malay Peninsula and Java, have mountainous terrain that partially
10 blocks low-level flow under typical environmental stratification. For east-
11 erly low-level flow, these terrain features often produce lee vortices, some of
12 which subsequently shed and move westward from the northern and south-
13 ern tips of Sumatra and thence downstream over the IO. Since Sumatra strad-
14 dles the equator, extending in a northwest-to-southeast direction from approx-
15 imately 6°N to 6°S , the lee vortices, while counter-rotating, are both cyclonic.
16 Hence, they have the potential to contribute to TC genesis over the northern
17 and southern IO. In addition, low-level, equatorial westerly flow impinging
18 on Sumatra is also typically blocked and diverges, at times contributing to cy-
19 clonic circulations over the IO primarily near the southern end of the island.

20 Data from two recent tropical campaigns, the 2008-10 Year of Tropical
21 Convection (YOTC) and the 2011 Dynamics of the Madden-Julian Oscilla-
22 tion or MJO (DYNAMO), are used to study these phenomena. These data sets
23 reveal the frequent occurrence of stationary and shed terrain-induced cyclonic
24 circulations over the IO, the majority of which occur during boreal fall and
25 winter when the MJO is active. During the 2.5 years of the two campaigns,
26 13 wake vortices (13% of the shed circulations identified) were tracked and
27 observed to subsequently develop into TCs over the northern and southern IO,
28 accounting for 25% of the total IO TCs during that period.

29 **1. Introduction**

30 A range of processes acting singly or in concert has been observed to contribute to tropical
31 cyclone (TC) genesis, e.g., African Easterly Waves (AEWs), convectively coupled equatorial
32 waves, breakdown of the intertropical convergence zone (ITCZ), monsoon troughs, and upper
33 level-troughs. It has also been proposed that topographic effects may influence TC genesis. This
34 possibility has been explored for the eastern Pacific Ocean by Farfán and Zehnder (1997) and
35 Zehnder et al. (1999). These studies found that easterly flow impinging upon zonally and diago-
36 nally oriented mountain ranges in Central America and Mexico can generate along-mountain jets
37 and lee vortices. These features then combine with AEWs and moist flow out of the ITCZ to
38 initiate tropical cyclogenesis.

39 This paper investigates another possible topographic influence on TC genesis, namely, the gen-
40 eration of vortices by the large cross-equatorial island of Sumatra and neighboring topographic
41 features. When stratified flow is blocked by an isolated obstacle, counter-rotating vortices may
42 form in its wake as flow diverts to either side of the barrier and converges downstream (Smolarkiewicz and Rotunno 1989; Rotunno and Smolarkiewicz 1991). When the Froude number, the
43 ratio of the approaching wind speed to the Brunt Väisälä frequency times the obstacle height, is
44 less than one, flow blocking is preferred. Generally, flow will be split or blocked below some crit-
45 ical height, and will flow over the obstacle above that critical height (Smolarkiewicz and Rotunno
46 1989). There can be a production of potential vorticity in the wake vortices if the flow surmounting
47 the barrier undergoes a hydraulic jump, along with an associated slight reduction in the surface
48 pressure (Schär and Smith 1993a; Epifanio and Durran 2002; Epifanio 2003). For elongated bar-
49 riers such as Sumatra, wave breaking, flow splitting, and the development of lee vortices depend
50 not only on the Froude number (the inverse of which is the non-dimensional mountain height) but
51

52 also on the horizontal aspect ratio of the barrier (the ratio of the cross-stream length scale to the
53 stream-wise length scale of the barrier) (Smith 1989; Epifanio 2003). For typical flow conditions
54 around many islands in the tropics and subtropics, lee vortices are commonplace. These vortices
55 often shed and move downstream as a result of boundary layer separation, perturbations in the
56 flow, or instability in the wake (Etling 1989; Schär and Smith 1993b). Sumatra is one such island
57 where the conditions for flow splitting and lee vortex formation are met.

58 In this study it is proposed that flow blocking and splitting by the topography on the island of
59 Sumatra and adjacent topographic features – the mountainous west end of Java and the Malay
60 Peninsula – can lead to TC genesis in the Indian Ocean. With respect to Sumatra, a narrow
61 mountain range stretches along its entire length, from approximately 6°N to 6°S, exceeding 3000
62 m in elevation near the island's northern tip (Fig. 1). Easterly wind blocked by the island will result
63 in wake vortices over the Indian Ocean in each hemisphere that will rotate in opposite directions,
64 but since the island straddles the equator, both are cyclonic. This unique situation is not found
65 elsewhere in the tropics. It is proposed that these wake vortices may then serve as pre-existing
66 cyclonic disturbances out of which TCs may develop. Such a possibility was first explored by
67 Kuettner and Soules (1967) and Kuettner (1989), who argued that the splitting of *easterly* flow by
68 Sumatra was responsible for sets of twin cyclones in the Indian Ocean and, using satellite imagery,
69 traced these TCs back to wake vortices observed downstream of Sumatra under low-level easterly
70 flow regimes.

71 However, it is evident from Fig. 1 that for easterly flow there are other islands and topographic
72 features in the maritime continent that can potentially have an impact on the circulation down-
73 stream over the Indian Ocean. As it turns out, the features other than Sumatra of greatest signif-
74 icance with respect to lee vortex generation affecting the Indian Ocean are the Malay Peninsula
75 and the island of Java. For the Malay Peninsula, it will be seen that easterly flow directed around

76 the Titiwangsa Mountains in the south and across the narrow island gap to the north can lead to lee
77 vortices that impinge upon or skirt the north end of Sumatra. On the other hand, southeasterly flow
78 impinging on the high terrain of west Java also leads to the generation of lee vortices downstream,
79 which upon shedding then pass the southern tip of Sumatra.

80 *Westerly* flow impinging on Sumatra may also result in downstream wake vortices, but these
81 are both anticyclonic and occur over the islands and inland seas of the maritime continent, so TC
82 genesis related to this flow blocking situation is not a possibility. However, given the high terrain
83 all along the western side of Sumatra (Fig. 1), blocking of equatorial westerly flow by the barrier
84 may also contribute cyclonic circulations *upstream* of the island as the flow splits at the equator
85 and moves north and south. This topographic effect will be seen to be yet another factor in TC
86 genesis over the Indian Ocean, thus expanding upon the idea originally advanced by Kuettner
87 (1989) regarding the blocking of low-level easterly flow by the island. There have been previous
88 studies of the blocking of westerly flow by Sumatra in the context of the passage of the MJO
89 (Inness and Slingo 2006; Wu and Hsu 2009) and convectively coupled Kelvin waves (Ridout and
90 Flatau 2011) over the maritime continent.

91 The potential for intensification of terrain-induced vortices into TCs over the eastern Indian
92 Ocean, is affected by seasonal and intraseasonal variability of the flow. As noted, easterly wind
93 impinging upon Sumatra may be blocked and generate cyclonic lee vortices in both hemispheres.
94 One source of low-level easterly wind in the Indian Ocean is the Madden-Julian Oscillation (MJO:
95 Madden and Julian 1971, 1972), which is the dominant mode of intraseasonal tropical variability
96 (e. g., Zhang 2005). In the Indian and western Pacific Oceans, the MJO is characterized by low-
97 level easterly winds preceding the arrival of an eastward-propagating convective envelope or active
98 phase, followed by low-level westerly winds. Wake vortices developing over the Indian Ocean
99 downstream of Sumatra in the easterly flow, once shed, may then traverse an environment with

100 enhanced moisture and divergence aloft, thus aiding TC genesis. Recently, Duvel (2015) showed
101 that the MJO enhances the frequency of TC genesis over the southern Indian Ocean by increasing
102 both the number of tropical depression initiations and the probability of their intensification. The
103 increased frequency is attributed to the MJO enhancing the cyclonic meridional shear of the zonal
104 wind in the TC genesis latitudes.

105 The Southeast Asian and Australian monsoons also exert an influence on tropical cyclogenesis
106 in the Indian Ocean basin. When the summer and winter monsoons are established, strong vertical
107 wind shear discourages tropical cyclogenesis (Gray 1968). During the transition period into the
108 winter monsoon, the vertical shear is reduced so that when the low-level flow is easterly, cyclonic
109 vortices that develop over the Indian Ocean west of Sumatra have a greater opportunity for eventual
110 intensification into a TC. Indeed, in the limited years that he analyzed, Kuettner (1989) observed
111 TCs intensifying out of wake vortices generated by Sumatra between October and December, and
112 in May, which represent the monsoon transition periods.

113 Synoptic and local-scale meteorological phenomena also complicate conditions associated with
114 wake vortices developing near Sumatra. Convectively coupled equatorial waves, such as equatorial
115 Rossby or Kelvin waves, have been shown to assist tropical cyclogenesis (Bessafi and Wheeler
116 2006; Frank and Roundy 2006; Roundy 2008; Schreck and Molinari 2009, 2011; MacRitchie
117 and Roundy 2012; Schreck 2015). In addition, there is frequently a pronounced diurnal cycle of
118 convection over and in proximity to Sumatra (e. g., Mori et al. 2004; Qian 2008; Wu et al. 2009).
119 This diurnal cycle may have a further influence on circulations that develop locally around the
120 island including their shedding and movement away from the barrier.

121 Analysis of terrain-induced vortex formation by topographic features in and around Sumatra and
122 its possible role in TC genesis are explored using datasets from two field campaigns: the 2008-
123 10 Year of Tropical Convection (YOTC) and the October-March 2011-12 Dynamics of the MJO

124 (DYNAMO) experiment. These campaigns were selected because of high-resolution analyses
125 available to detect topographically induced local circulations, as well as their subsequent passage
126 over the Indian Ocean.

127 **2. Data and Methods**

128 *a. Data*

129 The data for this study are from the YOTC and DYNAMO campaigns. YOTC was a “virtual”
130 field experiment, conducted between May 2008 and April 2010, with a focus on gathering and
131 assimilating existing sources of data, such as those from satellite observations or buoys, to better
132 understand and simulate many tropical phenomena (Moncrieff et al. 2012). There were six active
133 MJO events noted during YOTC, which passed by Sumatra in June and September 2008; February,
134 April, and November 2009; and April 2010 (Waliser et al. 2012). The active phases of the April
135 2009 and later MJO occurrences featured stronger convection, and remained intact and propagated
136 farther east than did the other YOTC MJO events (Waliser et al. 2012).

137 The DYNAMO campaign involved in-situ measurements by radiosonde, ship, and aircraft-based
138 instruments in the Indian Ocean basin, where the MJO typically initiates (Yoneyama et al. 2013;
139 Johnson and Ciesielski 2013). The special observing period (SOP), which featured the greatest
140 spatial and temporal density of observations, ran from 1 October to 15 December 2011, followed
141 by a period of less-intense observations through the end of March 2012. There were two MJO
142 events during the DYNAMO SOP, in October and November. The November MJO event was noted
143 for its strong convection, two westerly wind bursts, and the interaction of Kelvin waves, equatorial
144 Rossby waves, and nascent TC development over the northern Indian Ocean (Gottschalek et al.
145 2013; Judt and Chen 2014; Oh et al. 2015).

146 A reanalysis dataset for YOTC (1 May 2008 to 30 April 2010) and the operational analysis (OA)
147 dataset for DYNAMO (1 October 2011 to 31 March 2012) were produced by the European Centre
148 for Medium-range Weather Forecasting (ECMWF). These datasets were created by a component
149 of ECMWF's global model running at an enhanced resolution with observations during YOTC
150 and DYNAMO assimilated into the model (Moncrieff et al. 2012; Johnson and Ciesielski 2013).
151 For both datasets, the spatial resolution is 0.25° , with 18 pressure levels available between the
152 surface and 50 hPa, and the temporal resolution is 6-hourly. It should be kept in mind that the
153 YOTC period is two years, whereas the DYNAMO period is six months, so comparison of annual
154 distributions from the two campaigns is not possible.

155 As a proxy for convective activity, outgoing longwave radiation (OLR) data at 1° resolution from
156 the National Oceanic and Atmospheric Administration (NOAA) Earth System Research Labora-
157 tory (ESRL), Boulder, Colorado (www.esrl.noaa.gov/psd; Lee 2014) have been utilized.

158 Tropical cyclone track, intensity, and naming designations were obtained from best track data
159 from the Joint Typhoon Warning Center (JTWC) as well as from NOAA's International Best Track
160 Archive for Climate Science (IBTrACS) website (www.ncdc.noaa.gov/ibtracs).

161 *b. Methods and definition of analysis regions*

162 In order to determine the origin of terrain-induced circulations that ultimately led to TC genesis,
163 a procedure is needed to identify and track the circulation features. While most of the prominent
164 circulations can be identified and tracked subjectively, the limitations of such an approach as well
165 as the large number of cases during the 2.5 years of study, both stationary and shed circulations,
166 demands that an objective procedure be used. Hence, the identification and tracking of vortices
167 was carried out using the objective feature tracking code of Hodges (1995, 1999). While the
168 cyclonic circulation features were commonly associated with negative height anomalies, as shown

169 by Duvel (2015) for the southern Indian Ocean, many of the circulations tracked very close to
170 or even crossed the equator, which has led to the use of relative vorticity for tracking. Relative
171 vorticity fields at 6-h and 0.25° horizontal resolution from the YOTC analyses (May 2008 to April
172 2010) and ECMWF OA (October 2011 to March 2012) were vertically averaged over the 925-850
173 hPa layer, then smoothed to retain spatial scales greater than 450 km. Sensitivity test showed that
174 changes to the smoothing cutoff length had no notable impact on the identification of vortices.
175 The vertical averaging of vorticity was used to improve the temporal coherency of features when
176 a vorticity maximum shifts between different model levels (Serra et al. 2010). Cyclonic vorticity
177 features were tracked if their peak amplitude was greater than $1.0 \times 10^{-5} \text{ s}^{-1}$ and they persisted
178 for longer than 2 days. This threshold is larger than that used by Serra et al. (2010) for African
179 Easterly Waves, but sensitivity tests show that this value effectively captures significant vortex
180 features that have the potential to contribute to TC genesis.

181 To focus on vortex wakes that transitioned into Indian Ocean tropical storms, we restrict our
182 analyses only to cases in which the vortex shed westward over the Indian Ocean. To differentiate
183 between westward-shedding and stationary vortices, shed vortices are defined as those with (1) a
184 final location over the Indian Ocean that is > 500 km from Sumatra, and either (2) final minus
185 initial distance from Sumatra is > 250 km, or (3) their speed away from Sumatra is $> 0.5 \text{ m s}^{-1}$.
186 Condition (1) ensures that the shed vortex at the end of its track is some critical distance from
187 Sumatra and (2) or (3) ensure that it is moving away from this land mass.

188 Application of the tracking code to the 2.5 years of data yields information on both genesis lo-
189 cations and tracks of the cyclonic vortices. Genesis locations are shown in Fig. 2, separately for
190 the boreal cold (November-April) and warm (May-October) seasons. During the boreal winter
191 monsoon (Fig. 2a), northeasterly flow across the Malay Peninsula and the northern tip of Suma-
192 tra produces a high frequency of lee vortices just downstream of these topographic features. To

193 quantify relationships between the flow and downstream circulations in these regions (to be shown
194 later), two analysis boxes are defined in Fig. 2a: SN (Sumatra north) and MP (Malay Peninsula).
195 There are also genesis maxima across the northern parts of Sri Lanka and the Western Ghats, as
196 well as a broad area of genesis sites (unrelated to topography) in the southern ITCZ (Duvel 2015).

197 During the boreal summer monsoon, southeasterly flow across west Java and the southern tip of
198 Sumatra leads to two genesis maxima in those locations (Fig. 2b). Regions SS (Sumatra south)
199 and JV (Java), defined for later analyses, encompass these maxima. Similar to SN and MP, these
200 regions are downstream of the relevant topographic features, indicating the majority are wake
201 vortices. There are also maxima at the southern tip of India and southeast of Sri Lanka, as well as
202 through a gap in the Bukit Barisan mountain range on Sumatra. However, these maxima, as well
203 as those over India and Sri Lanka in the cold season, do not contribute to TC genesis, so they will
204 not be considered in our analysis.

205 To delineate easterly and westerly flow regimes, which determine where terrain-induced vortices
206 will form and move in relation to the topography, two computation line segments are identified in
207 Fig. 1 ($3-7^{\circ}\text{N}$, 100°E and $3-7^{\circ}\text{S}$, 105°E). Averages of the zonal wind along these lines (defined as
208 U_N and U_S , respectively) are considered representative of the flow in the analysis boxes adjacent
209 to them. To determine the likelihood of flow blocking or splitting by the topographic features in
210 the regions, Froude numbers were evaluated in proximity to these line segments using zonal wind
211 speed and Brunt-Väisälä frequency averaged over the 950-850 hPa layer and assuming average
212 terrain heights of 1 and 0.5 km in the north and south, respectively.

213 To identify convectively coupled equatorial waves and their relationship to the wake vortices
214 and TC genesis, OLR anomalies were calculated from the NOAA OLR data, then filtered for
215 different wave mode characteristics – period, wavenumber, and equivalent depth (Wheeler and

216 Kiladis 1999) – which identify Kelvin, equatorial Rossby, MJO-type, or mixed-Rossby gravity
217 waves (code provided by K. Straub, 2014, personal communication).

218 **3. Results**

219 *a. Vortex statistics and tracks*

220 Terrain-induced vortices that moved westward out over the Indian Ocean and had the potential
221 to contribute to TC genesis originated in the four analysis boxes shown in Fig. 2. Therefore, these
222 regions are identified as the focal areas for subsequent analyses. Statistics on shed and non-shed
223 (i.e., more or less stationary) vortices from these four regions are presented in Table 1. A total of
224 309 cyclonic vortices were detected in the four regions during the 2.5 years of data, 103 (33%) of
225 which were shed, i.e., moved downstream away from their point of origination. The vast majority
226 (90%) of the shed circulations from Sumatra north (SN) and the Malay Peninsula (MP) occurred
227 during easterly flow, hence were lee or wake vortices that detached from the terrain features. A
228 similar high percentage (95%) of shed vortices occurred along west Java (JV) in easterly flow.
229 The frequency for Sumatra south (SS) during easterly flow (72%) was somewhat less, indicating a
230 fair number of cases of westerly flow impinging on Sumatra contributing to cyclonic circulations
231 off the southern tip of the island. Flow conditions associated with shedding in all regions will be
232 shown in the next subsection.

233 Also indicated in Table 1, there were 13 terrain-induced vortices that subsequently developed
234 into named TCs: five from SN, six from SS, and two from JV. Tracks and other information
235 pertaining to these events will be shown later; however, a summary of these 13 events and their
236 relationship to the total named tropical cyclone counts in the Indian Ocean basin¹ for the various

¹The Indian Ocean basin is defined here as that portion of the Indian Ocean extending from Africa to 105°E; hence, it excludes the tropical cyclone formation zone along the northwest coast of Australia.

237 YOTC and DYNAMO time periods is shown in Table 2. The five TCs over the northern IO
238 originating from terrain-induced circulations represent 29% of the total (17) TCs in the northern
239 hemisphere during the 2.5-year period, whereas the eight TCs similarly identified for the southern
240 IO represent 24% of the total (34) for that region. *Notably, for the entire IO basin, the 13 TCs*
241 *originating from shed vortices represent 25% of the total (51) TCs occurring in the Indian Ocean*
242 *basin during the period of study, highlighting the important role of topography in TC genesis in*
243 *this region.* Moreover, these percentages likely represent a lower bound to such events since they
244 include only cases in which the tracking program provided conclusive evidence of a wake to TC
245 transition. Other cases may not have been captured to due limitations in the reanalysis datasets
246 and those imposed by the various tracking procedure settings (e.g., a lower vorticity amplitude
247 threshold may have yielded longer, more continuous tracks).

248 The monthly distributions of the shed and non-shed vortices, as well as TCs originating from
249 terrain-induced circulations, for regions SN and MP are shown in Fig. 3. Values are shown in
250 counts per year to take into account the fact that the data records for YOTC (two years) and
251 DYNAMO (six months) are different. From Fig. 3 it is seen that cyclonic vortices generated by
252 the topographic features in SN and MP occur predominantly during the boreal winter monsoon,
253 when low-level easterly flow prevails over the region (Figs. 2a and 3c). Shedding of vortices is
254 more common from SN than MP (Table 1), and only SN-shed vortices (five cases in October and
255 November, representing 12% of the shed events) led to TC genesis during the 2.5 years of study.

256 Cyclonic vortices from regions SS and JV are distributed somewhat more broadly throughout the
257 annual cycle (Fig. 4), although the majority occurred during the austral winter and spring seasons.
258 On average, the flow across these terrain features during this period had an easterly component
259 (Figs. 2b and 4c). However, unlike the northern Sumatra region, those terrain-induced cyclonic
260 vortices that led to TC genesis occurred under conditions of both mean easterly and westerly flow.

261 With respect to timing, most TC cases (5 out of 8) in the southern Indian Ocean occurred during
262 the boreal winter monsoon, as was the case in region SN.

263 To further emphasize the importance of the topography surrounding the Indian Ocean basin for
264 initiating cyclonic circulations, a map of all vortex tracks originating between 10°N and 10°S
265 in this region during the 2.5 years of data is shown in Fig. 5. The role of significant terrain
266 features – Sumatra, the Malay Peninsula, west Java, southern India, and Sri Lanka – for generating
267 cyclonic circulations is clearly evident. Many of the circulations produced by SN and MP move
268 due westward, whereas those from SS and JV are frequently swept northwestward off the southern
269 coast of Sumatra by the southeasterly flow (Fig. 2b). Tracks emanating from Sri Lanka and the
270 south tip of India occur predominantly during the fully developed winter and summer monsoons
271 and do not contribute to TC genesis due to stronger vertical shear during these periods.

272 The tracks of the cyclonic circulations emanating from the four analysis boxes are shown in Fig.
273 6. Most tracks extend westward over the Indian Ocean and, hence, potentially can contribute to
274 TC genesis. Indeed, a number of the tracks, including some spanning most of the entire Indian
275 Ocean, eventually became named TCs (as will be shown later).

276 As mentioned earlier, shedding of wake vortices may be a result of boundary layer separation,
277 perturbations in the flow, or instability in the wake (Etling 1989; Schär and Smith 1993b). Compar-
278 ison of the mean lower-tropospheric flow for shed and non-shed vortices (easterly flow cases only)
279 for region SN (Fig. 7) reveals rather subtle flow differences across the northern tip of Sumatra.
280 Specifically, shed events have a slightly stronger easterly flow to the north of the island, perhaps
281 aiding the shedding process. Furthermore, additional analyses of the SN cases (not shown), in-
282 dicate that for shed cases, easterly flow in the vicinity of SN increases and peaks one to two
283 days following the initiation date of the wake vortex, whereas for non-shed cases, easterly flow
284 diminishes following wake vortex initiation.

285 The mean flow for shed cases for region SS for both easterly and westerly flow is shown in Fig.
286 8. Cyclonic vortex generation over the eastern Indian Ocean south of the equator in easterly flow
287 (Fig. 8a) is in part created by southeasterly flow against the mountain barrier along the southern
288 part of the island. However, in addition, blocking of westerly flow along and just to the north of
289 the equator by the island is seen to partially contribute to the cyclonic circulation in this region.
290 This effect is particularly noticeable for westerly flow in region SS (Fig. 8b), where upstream
291 blocking and splitting of equatorial westerly flow is seen to contribute to cyclonic circulations in
292 both hemispheres.

293 *b. Vorticity production by topography*

294 Topographically generated vorticity streamers, similar to “PV banners” investigated during the
295 Mesoscale Alpine Programme (Aebischer and Schär 1998), are seen to be commonplace throughout
296 the Asian-Australian monsoon region (Fig. 9). To illustrate this behavior, streamlines and relative
297 vorticity averaged for the six-month DYNAMO period are shown in Fig. 9a for easterly 925-850
298 hPa flow having a magnitude exceeding 5 m s^{-1} averaged along the northern line segment in Fig.
299 1. A positive vorticity maximum is observed at the northern tip of Sumatra, consistent with the
300 observation of frequent vortex generation just downstream (Fig. 2a). A streamer of vorticity ex-
301 tends due westward into the Indian Ocean, suggestive of frequent shedding of these vortices. The
302 average Froude number (Fr) in the 950-850 hPa layer under the easterly flow regimes was ~ 0.3 ,
303 supporting flow blocking and splitting by Sumatra’s mountains (Smith 1989; Smolarkiewicz and
304 Rotunno 1989). Positive vorticity is also observed downstream of the northern periphery of other
305 islands in the maritime continent such as Borneo, the island of Sri Lanka, and significant topo-
306 graphic features elsewhere in the region. Negative geopotential height anomalies were observed

307 in the center of these cyclonic vortices (not shown here, but illustrated later), consistent with the
308 findings of Schär and Smith (1993b).

309 For the flow conditions used to produce Fig. 9a, cyclonic vorticity can also be seen downstream
310 of the southern tip, with a closed circulation offshore extending into a broad expanse of negative
311 vorticity across most of the Indian Ocean between the equator and 10°S .² This broad trough re-
312 gion reflects the existence of the southern Indian Ocean ITCZ. Froude numbers associated with
313 easterly flow for the southern regions were ~ 0.7 , suggesting a slightly weaker blocking effect by
314 the southern portion of the island, principally due to the lower average topography there (Fig. 1).

315 During low-level westerly flow across the northern tip of Sumatra, anticyclonic relative vorticity
316 was observed along Sumatra's northern tip (Fig. 9b), as well as to the lee of the Malay Peninsula
317 and at the north coast of Borneo. During this period, the southern ITCZ (indicated by cyclonic or
318 negative vorticity) was still present, though shifted slightly equatorward.

319 To better quantify the relationship between zonal wind and the circulation downstream of Suma-
320 tra, relative vorticity (averaged within one of the analysis regions) was regressed onto zonal wind
321 (averaged along the northern or southern line segment in Fig. 1) at different levels in the lower
322 troposphere. Peak correlations were found to occur in the height range from 925 to 850 hPa level
323 in the north and at 1000 hPa in the south, with correlations dropping off at higher levels (Fig. 10).
324 This behavior is consistent with expected flow blocking for topography with an average height
325 of 1-2 km in the northern Sumatra region and somewhat lower in the south. Considering these
326 findings, a level of 900 hPa is chosen to illustrate correlations between zonal wind and relative
327 vorticity for all four regions (Fig. 11). For the entire 2.5 year period, cyclonic (positive) vorticity
328 in regions SN and MP (Fig. 11, top panels) was negatively correlated to the zonal wind (all corre-

²The flow pattern illustrated in Fig. 9a closely resembles that depicted by Kuettner (1989) as an archetype of the circulation associated with twin cyclone development in the eastern Indian Ocean, leading him to propose Sumatra as a potential generator of incipient TC disturbances.

329 lations significant at the 99% level). In other words, the stronger the oncoming flow, the stronger
330 the vorticity in the analysis regions.

331 In regions SS and JV (Fig. 11, bottom panels), correlations between 900-hPa zonal wind and
332 relative vorticity were poorer than those for the northern regions. This is not unexpected since
333 the average topography is lower in the south (Fig. 1). In addition, the mean vorticity is nearly
334 always cyclonic off the southwest coast of Sumatra due to the relatively persistent ITCZ, which
335 migrates north and south throughout the year (Fig. 2). The persistence of cyclonic vorticity near
336 southern Sumatra regardless of flow direction is evident in Fig. 11 (bottom panels) where most of
337 the relative vorticity values are negative for easterly flow cases and the majority are also negative
338 for westerly flow cases.

339 *c. Vortex shedding and tropical cyclone genesis*

340 Once formed, lee vortices often shed and move downstream, as dramatically illustrated in satel-
341 lite images of wake circulations in fields of stratocumulus to the lee of mountainous islands
342 (Chopra and Hubert 1965; Etling 1989; Schär and Durran 1997). In the case of Sumatra, stra-
343 tocumulus clouds are not present to define the wake circulations; nevertheless, the circulations do
344 exist based on the quarter degree reanalysis data. The shedding of vortices has been related to
345 viscous boundary layer separation (Etling 1989) or absolute instability of the symmetrical wake
346 (Schär and Durran 1997). Creation of potential vorticity (PV) in the wake circulation has been
347 attributed to dissipation in hydraulic jumps associated with flow over the barrier or dissipation in
348 the wake (Schär and Smith 1993a; Smith and Grubišić 1993; Epifanio and Durran 2002). Once
349 created, the PV anomaly can persist as it moves downstream, unless acted upon by dissipative
350 processes.

351 The formation and downstream movement of lee vortices for the latitudes of both northern and
352 southern Sumatra are shown for the YOTC and DYNAMO years in the wind-vorticity Hovmöller
353 diagrams shown in Figs. 12-14. All of the TCs traced back to wake vortices generated by Suma-
354 tra's topography in the *northern* Indian Ocean during the YOTC and DYNAMO periods occurred
355 during the months of OND (Fig. 3). During the OND periods for all three years, positive vortic-
356 ity maxima at 850 hPa frequently occur near 95°E in region SN just west of Sumatra's northern
357 tip (Figs. 12a, 13a, and 14a; central longitude of Sumatra indicated by dashed line). Similarly,
358 in Figs. 12-14, frequent vorticity maxima can also be seen at the longitudes of the other regions:
359 MP (~100-102°E), SS (~100°E), and JV (~105°E). Farther east, other positive/negative vorticity
360 anomalies are evident and associated with terrain features in the maritime continent (Fig. 9a).

361 The common occurrence of positive vorticity maxima at the longitude of Sumatra's northern tip
362 (also seen in Figs. 13a and 14a during easterly flow) is evidence of persistent lee vortex formation.
363 On occasion, however, the positive vorticity anomalies detach from Sumatra and move westward.
364 Three instances of such events directly associated with TC development are depicted in Fig. 12a:
365 TC 03A in October, Nisha in November, and TC 07B in December.³

366 A similar pattern of cyclonic (negative) vorticity maxima near 95°E just west of Sumatra's south-
367 ern tip is seen in Fig. 12b (fields are at 925 hPa due to lower topography there) although its asso-
368 ciation solely with easterly flow is less obvious than in northern Sumatra. One westward-moving
369 vorticity streamer in October was a precursor to TC Asma, the southern Indian Ocean counterpart
370 to TC 03A.

371 During the 2009 OND YOTC period, vorticity maxima once again occurred near Sumatra's
372 northern tip associated with lee vortex formation, and several instances of shedding vortices were

³In the case of TC 03A and several others shown later, the location of the storm symbol is displaced outside the vorticity streamer in the time-longitude diagrams since the official naming of the TC occurred when the center was outside the 3-7° latitude band.

373 evident in November (Fig. 13a). However, TC Ward was the only northern Indian Ocean storm
374 during the OND 2009 period to develop from a lee vortex. Over the southern Indian Ocean, TCs
375 Cleo and David (Fig. 13b) formed around the time of TC Ward, collectively constituting cross-
376 equatorial “triplets” in December 2009. Cleo and David both reached tropical storm wind speeds
377 following the end of vorticity streamers depicted within the southern Sumatra latitude band (Fig.
378 13b), although it is difficult to identify each storm with a particular shed vortex in this depiction
379 since the wake vortices moved out of the 3-7°S latitude band before intensifying. The continuity of
380 these circulations will become more apparent in the discussion of individual cases in the following
381 subsection.

382 During the DYNAMO year, the three instances where wake vortices propagated westward and
383 became tropical cyclones – TC 05A in the northern hemisphere and TCs Alenga and Benilde in
384 the southern hemisphere – are indicated in Fig. 14. There are also a number of shed wake vortices
385 (vorticity streamers) in both hemispheres that did not develop into tropical cyclones. However,
386 two of the TCs that developed, 05A and Alenga, moved into a favorable environment for TC
387 genesis provided by the developing MJO over the central Indian Ocean (Yoneyama et al. 2013;
388 Gottschalck et al. 2013). Prominent vorticity maxima immediately to the west of Sumatra’s tips
389 regularly occurred during periods of low-level easterly flow at 850 hPa in both the northern (Fig.
390 14a) and southern (Fig. 14b) hemispheres, with westward movement of streamers in a number of
391 instances.

392 Results for the YOTC and DYNAMO years indicate that when easterly wind was sustained
393 upon Sumatra, multiple wake vortices were observed to form and propagate away in succession.
394 This can be seen in November 2009 (Fig. 13a), and in the easterly wind periods that preceded the
395 late October and November 2011 MJO events (Fig. 14a). In some instances, as will be evident
396 in the cases presented later, augmentation of cyclonic vorticity appeared to occur when *westerly*

397 equatorial wind impacted central Sumatra as well. In these situations the high terrain on the
398 western side of Sumatra blocked low-level equatorial westerly flow, diverting it to the north and
399 south, so that when combined with easterly flow across Sumatra's tips, cyclonic vorticity was
400 enhanced in those locations.

401 The southern Indian Ocean near Sumatra demonstrated a prominent secondary maximum in vor-
402 ticity streamer frequency between March and May (not shown), another period of climatologically
403 frequent tropical cyclogenesis in the Indian Ocean. Five out of eight TCs determined to have orig-
404 inated from Sumatran wake vortices in the southern Indian Ocean during YOTC and DYNAMO
405 developed between October and December. The other three developed in the austral summer,
406 January and March.

407 In total, ten TCs during YOTC, and three during DYNAMO, were determined to have intensified
408 from wake vortices that formed downstream of Sumatra. Three TCs, Gael (2009) during YOTC
409 and 05A and Alenga (2011) during DYNAMO, formed in the easterly flow regimes preceding the
410 active phase of MJO events. The tracks of all of the wake vortices that eventually developed into
411 tropical cyclones during the two years of YOTC and the DYNAMO SOP are plotted in Fig. 15.
412 The pre-TC periods of the tracked vortices are marked by thin lines, the named-storm periods by
413 thick lines. Some wake vortices remained coherent and traversed most of the Indian Ocean basin
414 before they intensified and were named by the responsible agencies, while others intensified quite
415 close to Sumatra. Three sets of cross-equatorial, companion tropical cyclones that originated from
416 wake vortices during the analyzed time periods were TCs 03A and Asma in October 2008; TCs
417 Cleo, Ward, and David in December 2009; and TCs 05A and Alenga in late November and early
418 December 2011.

419 The 13 TCs identified to have originated from terrain-induced circulations during YOTC and
420 DYNAMO are listed in Table 3. The length of time from vortex genesis to naming of the storms

421 by operational centers ranged from 5 to 20 days, with an average duration of 10.1 days, indicating
422 a long gestation period for many of the disturbances prior to TC genesis. Comparing results from
423 Tables 1 and 2, 9% (18%) of the vortices identified using the vorticity threshold of 1.0×10^{-5}
424 s^{-1} that shed from the northern (southern) regions of Sumatra eventually became named TCs.
425 As mentioned earlier, these TCs comprised nearly one-quarter of all TCs occurring in the Indian
426 Ocean basin during the period of study.

427 *d. Selected case studies*

428 The genesis of tropical cyclones 07B (2008), Cleo, Ward, and David (2009), and 05A (2011),
429 have been selected to illustrate wake vortex development, associated geopotential height falls,
430 and subsequent transformation into TCs. Detailed mechanisms involved in their transformations
431 cannot be fully determined from the available data, so this aspect of their life cycles is beyond
432 the scope of this study. The full tracks of the TCs, beginning as wake vortices near Sumatra, are
433 shown in Fig. 15.

434 TC 07B was a lone wake vortex and tropical cyclone in the northern Indian Ocean in December
435 2008. During late November 2008, easterly wind impacted the northern tip of Sumatra and gen-
436 erated a wake vortex (Fig. 16a-c). In this case, positive vorticity was also observed upstream of
437 the island as easterly flow impinged on Borneo, as illustrated in the time-longitude plot of 850-
438 hPa vorticity (Fig. 12a). However, a closed circulation upstream of Sumatra was not present (not
439 shown). Geopotential height falls at 850 hPa were already evident in the vortex on November 29.
440 Prevailing winds along and south of the equator and against the island's southern tip were west-
441 erly while the vortex spun up. Cyclonic shear existed where the equatorial westerlies bordered
442 trade easterlies north of the equator (Fig. 16). TC 07B moved slowly northwestward and reached
443 tropical storm intensity on December 4, when the storm was officially named (Fig. 16d-f).

444 TCs Cleo, Ward, and David were “triplets” in December 2009. The wake vortex precursor to
445 TC Cleo in the southern hemisphere appeared to be assisted by blocking of westerly equatorial
446 flow by central Sumatra in late November 2009. The vortex is near 100°E on 2 December with
447 lower geopotential heights already at its center (Fig. 17a). Cleo eventually became a named storm
448 on 7 December. At the same time, a lee vortex appeared on the north end of the island, which
449 would eventually become TC Ward on 11 December (Figs. 15 and 17b-c). Low-level flow near
450 southern Sumatra shifted to easterly on 3 December and resulted in a second cyclonic wake vortex
451 in the southern Indian Ocean, which would later move westward and intensify into TC David (Fig.
452 17e-f), which was named on 13 December. In the cases of all three storms, no apparent upstream
453 cyclonic vorticity maxima were present prior to the wake vortex initiation (Fig. 13). Strong ($u > 7$
454 m s^{-1}) low-level equatorial westerlies were present over the eastern Indian Ocean through the
455 lifecycle of these burgeoning wake vortices, which, together with low-level trade easterlies farther
456 poleward, constituted cyclonic shear in both hemispheres. At their peak intensities, TCs Cleo and
457 Ward had estimated winds up to 115 and 45 kt, respectively. TC David reached the middle of the
458 Indian Ocean before intensifying to a maximum wind speed of 55 kt. Its remnants dumped heavy
459 rain on Mauritius and Reunion, causing flooding and damage (La Sentinelle 2009). There was
460 not an MJO event prior to TC 07B in December 2008, nor prior to TCs Cleo, Ward, and David,
461 to create environmental conditions that may have enhanced the potential for TC genesis, as in the
462 2011 (DYNAMO) cases of TC 05A and Alenga, which will be discussed next.

463 In late-November 2011, the wake vortex that would later become TC 05A initiated off the north
464 tip of Sumatra as easterly flow impinged upon the island (Fig. 18a). These easterlies were as-
465 sociated with the pre-onset phase of the approaching November 2011 MJO convective envelope
466 (Johnson and Ciesielski 2013). The vortex moved slowly westward over the next four days (Fig.
467 18c-f), but was not officially designated TC 05A until 26 November when it was west of Sri Lanka

468 and had encountered the moist MJO convective envelope. Though its maximum wind speed was
469 only 35 kt, it caused damage and deaths in Sri Lanka (Agence France-Presse 2011). The wake
470 vortex that would become TC Alenga formed ten days after the TC 05A vortex and therefore is
471 not depicted in Fig. 18, though it too interacted with the MJO convective envelope (in a way likely
472 similar to that described by Duvel 2015) to assist in its development, namely, by encountering
473 enhanced north-south shear of the low-level zonal flow.

474 The development of TC 05A was also influenced by convectively coupled equatorial waves,
475 which occurred in association with the late November 2011 active MJO event (Gottschalck et al.
476 2013; Oh et al. 2015). A convectively coupled equatorial Rossby (ER) wave moved westward
477 and passed over the vorticity streamer that represents the wake vortex precursor to TC 05A in late
478 November (Fig. 19a). The initiation of the vorticity streamer around 22 November was nearly
479 coincident with the arrival of the ER wave at the longitude of Sumatra. However, investigation of
480 all the other cases with respect to the passage of equatorial waves (equatorial Rossby and mixed-
481 Rossby gravity) did not show any consistent or systematic pattern of vortex shedding in association
482 with the waves (not shown). In addition, a Kelvin wave convective envelope, which featured strong
483 OLR anomalies, propagated eastward over the same region in late November 2011 (Fig. 19b). Its
484 encounter with the wake vortex on 25 November led to a pronounced strengthening of the vorticity
485 at that time. Strong westerly wind bursts, apparent in Figs. 18e and f, associated with the Kelvin
486 waves likely served to enhance the vortex's low-level cyclonic circulation. Gottschalck et al.
487 (2013) and Oh et al. (2015) describe the combined influence of Kelvin, equatorial Rossby, and
488 mixed-Rossby waves on the flow in the region of the developing TC 05A during this period.

489 **4. Summary and conclusions**

490 This study explores the potential role of the island of Sumatra and adjacent topographic features
491 in creating terrain-induced circulations over the Indian Ocean that later develop into tropical cy-
492 clones (TCs). Sumatra, as well as adjacent Malay Peninsula and Java, have mountainous terrain
493 that partially blocks low-level flow under typical environmental stratification. For easterly low-
494 level flow, these terrain features often produce lee vortices, some of which subsequently shed and
495 move westward from the northern and southern tips of Sumatra and thence downstream over the
496 Indian Ocean. Since Sumatra straddles the equator, extending in a northwest-to-southeast direction
497 from approximately 6°N to 6°S, the lee vortices generated at the two ends, while counter-rotating,
498 are both cyclonic. This unique situation is not found elsewhere in the tropics. The generation of
499 TCs by Sumatra wake vortices was first proposed many years ago by Kuettner and Soules (1967)
500 and Kuettner (1989), although little attention has been given to it since.

501 To investigate this problem, data from the 2008-10 Year of Tropical Convection (YOTC) and
502 2011-12 Dynamics of the MJO (DYNAMO) campaigns are used. ECMWF quarter degree reanal-
503 ysis and operational datasets from these campaigns have provided sufficient resolution to detect
504 and track the wake vortices that were observed to develop at the northern and southern ends of
505 Sumatra. The identification and tracking of vortices was carried out using the objective feature
506 tracking code of Hodges (1995, 1999). In applying this algorithm to the Indian Ocean basin, it
507 was discovered that in addition to Sumatra, the Malay Peninsula and the mountains of west Java
508 also contribute to cyclonic vortex development with eventual shedding of vortices into the Indian
509 Ocean where they have the potential to influence TC genesis. Therefore, attention is focused on
510 these two regions in addition to Sumatra itself with respect to topographic influence on the flow.
511 The majority of the shed circulations from both northern and southern Sumatra regions occurred in

512 easterly low-level flow, hence were lee or wake vortices. However, some instances of blocking and
513 splitting of low-level westerly equatorial flow by the mountainous island of Sumatra contributed
514 to cyclonic circulations *upstream* of the island.

515 Key findings of this study are as follows:

- 516 1. Sumatra and adjacent Malay Peninsula and west Java are prolific generators of low-level topo-
517 graphically induced circulations, contributing during YOTC and DYNAMO to 309 cyclonic
518 circulations having an amplitude threshold of $1.0 \times 10^{-5} \text{ s}^{-1}$ trackable over at least a two-day
519 period. Of these, 33% were shed, i.e., moved downstream from their point of origination.
- 520 2. During the 2.5 years of the two campaigns, 13 TCs (five in the northern hemisphere and eight
521 in the southern hemisphere) originated from shed vortices, representing 25% of all the TCs
522 occurring in the Indian Ocean basin during the period of study, indicating the important role
523 of topography in TC genesis in the region.
- 524 3. For shed vortices that eventually became TCs, the average length of time from vortex genesis
525 to the naming of the storms was 10.1 days, indicating a relatively long gestation period for
526 these TC precursor disturbances.

527 Though terrain-induced vortices occurred throughout much of the year, the occurrence of TC
528 genesis was in most cases (10 out of 13) confined to the October-December period due to the
529 low environmental vertical wind shear as the monsoon transitions from boreal summer to winter.
530 The results are consistent with those of Kuettner (1989), who found that all but one twin TC case
531 described in his study developed between October and December.

532 In four of the cases during YOTC and DYNAMO, easterly winds preceding the onset of the
533 MJO's active phase encountered Sumatra, producing cyclonic wake vortices that formed and
534 moved westward, subsequently interacting with the MJO convective envelope before develop-

535 ing into tropical storms. In the TC 05A case that occurred during DYNAMO, both the MJO and
536 equatorial waves (equatorial Rossby, mixed-Rossby gravity, and Kelvin waves) appeared to con-
537 tribute to the development of the TC (Gottschalck et al. 2013; Judt and Chen 2014; Oh et al. 2015),
538 although these studies did not indicate the potential role of Sumatra wake vortices in providing the
539 initial disturbance for the TC. Equatorial waves may have supported tropical cyclogenesis by pro-
540 ducing low-level cyclonic vorticity and lowering vertical wind shear, as detailed in other studies
541 (e. g., Frank and Roundy 2006), although the specifics of those processes have not been investi-
542 gated here.

543 This study has provided further evidence for the idea first proposed by Kuettner and Soules
544 (1967) and Kuettner (1989) that Sumatra may serve as a generator of wake vortices that subse-
545 quently develop into tropical cyclones. It has also been found, however, that the adjacent topogra-
546 phy on the Malay Peninsula and west Java is an important contributor to terrain-induced vortices
547 that move out over the Indian Ocean. Not all wake vortices develop into TCs, of course, since
548 favorable environmental conditions are required for TC genesis to occur. The MJO and equatorial
549 waves may provide those favorable conditions, though they are not a prerequisite for TC genesis.
550 These observational findings motivate numerical simulations to further explore the mechanisms
551 for this unique role of topography in TC genesis over the Indian Ocean.

552 *Acknowledgments.* We are indebted to Kevin Hodges of the University of Reading for providing
553 his tracking code for our study and his assistance in setting it up for our application. We also
554 thank Kathy Straub for providing the code for identifying convectively coupled equatorial wave
555 modes. The DYNAMO operational and YOTC reanalysis data sets were made available by the Eu-
556 ropean Centre for Medium-Range Weather Forecasts. This work has been supported by National

557 Science Foundation grants AGS-1059899, AGS-1138353 and AGS-136027, a one-year American
558 Meteorological Society Fellowship awarded to Caitlin Fine, and the United States Navy.

559 **References**

560 Aebischer, U., and C. Schär, 1998: Low-level potential vorticity and cyclogenesis to the lee of the
561 Alps. *J. Atmos. Sci.*, **55**, 186–207.

562 Agence France-Presse, 2011: Sri Lanka storm kills 19, damages 5700 homes. [Available online at
563 <http://www.webcitation.org/63Vnhm01u>].

564 Bessafi, M., and M. C. Wheeler, 2006: Modulation of South Indian Ocean tropical cyclones by
565 the Madden-Julian Oscillation and convectively coupled equatorial waves. *Mon. Wea. Rev.*, **134**,
566 638–656.

567 Chopra, K. P., and L. F. Hubert, 1965: Mesoscale eddies in the wake of islands. *J. Atmos. Sci.*, **22**,
568 652–657.

569 Duvel, J. P., 2015: Initiation and intensification of tropical depressions over the southern Indian
570 Ocean: Influence of the MJO. *Mon. Wea. Rev.*, **143**, 2170–2191.

571 Epifanio, C. C., 2003: Lee vortices. *Encyclopedia of Atmospheric Sciences*, J. R. Holton, J. Pyle,
572 and J. A. Curry, Eds., Elsevier Science Ltd., 1150–1160.

573 Epifanio, C. C., and D. R. Durran, 2002: Lee-vortex formation in free-slip stratified flow over
574 ridges. Part I: Comparison of inviscid theory and fully nonlinear viscous simulations. *J. Atmos.*
575 *Sci.*, **59**, 1153–1165.

576 Etling, D., 1989: On atmospheric vortex streets in the wake of large islands. *Meteorology and*
577 *Atmospheric Physics*, **41**, 157–164.

578 Farfán, L. M., and J. A. Zehnder, 1997: Orographic influence on the synoptic-scale circulations
579 associated with the genesis of Hurricane Guillermo (1991). *Mon. Wea. Rev.*, **125**, 2683–2698.

580 Frank, W. M., and P. E. Roundy, 2006: The role of tropical waves in tropical cyclogenesis. *Mon.*
581 *Wea. Rev.*, **134**, 2397–2417.

582 Gottschalck, J., P. E. Roundy, C. J. Schreck III, A. Vintzileos, and C. Zhang, 2013: Large-scale
583 atmospheric and oceanic conditions during the 2011–12 DYNAMO field campaign. *Mon. Wea.*
584 *Rev.*, **141**, 4173–4196.

585 Gray, W. M., 1968: Global view of the origin of tropical disturbances and storms. *Mon. Wea. Rev.*,
586 **96**, 669–700.

587 Hodges, K., 1995: Feature tracking on the unit sphere. *Mon. Wea. Rev.*, **123**, 3458–3465.

588 Hodges, K., 1999: Adaptive constraints for feature tracking. *Mon. Wea. Rev.*, **127**, 1362–1373.

589 Inness, P., and J. Slingo, 2006: The interaction of the Madden-Julian Oscillation with the Maritime
590 Continent in a GCM. *Quart. J. Roy. Meteor. Soc.*, **132**, 1645–1667.

591 Johnson, R. H., and P. E. Ciesielski, 2013: Structure and properties of Madden–Julian oscillations
592 deduced from DYNAMO sounding arrays. *J. Atmos. Sci.*, **70**, 3157–3179.

593 Judt, F., and S. S. Chen, 2014: An explosive convective cloud system and its environmental condi-
594 tions in MJO initiation observed during DYNAMO. *J. Geophys. Res. Atmos.*, **119**, 2781–2795.

595 Kuettner, J., 1989: Easterly flow over the cross equatorial island of Sumatra and its role in the
596 formation of cyclone pairs over the Indian Ocean. *Wetter und Leben*, **41**, 47–55.

597 Kuettner, J., and S. Soules, 1967: Types and scales of equatorial circulations as revealed from
598 space and their possible exploration by tropical field projects. *Proc. 5th Technical Conference*
599 *on Hurricanes and Tropical Meteorology*, Caracas, Venezuela, Royal. Meteor. Soc.

600 La Sentinelle, 2009: Pluies diluviennes: les pompiers et la Special Mo-
601 bile Force en état d’alert. [Available online at [http://www.lexpress.mu/article/
602 pluies-diluviennes-les-pompiers-et-la-special-mobile-force-en-%C3%A9tat-d%E2%80%
603 99alerte/](http://www.lexpress.mu/article/pluies-diluviennes-les-pompiers-et-la-special-mobile-force-en-%C3%A9tat-d%E2%80%99alerte/)].

604 Lee, H.-T., 2014: Outgoing Longwave Radiation (OLR) - Daily. NOAA’s Climate Data Record
605 (CDR) program. Climate algorithm theoretical basis document (c-atbd), National Center for
606 Atmospheric Research, Boulder, CO, 46 pp.

607 MacRitchie, K., and P. E. Roundy, 2012: Potential vorticity accumulation following atmospheric
608 Kelvin waves in the active convective region of the MJO. *J. Atmos. Sci.*, **69**, 908–914.

609 Madden, R. A., and P. R. Julian, 1971: Detection of a 40-50 day oscillation in the zonal wind in
610 the tropical Pacific. *J. Atmos. Sci.*, **28**, 702–708.

611 Madden, R. A., and P. R. Julian, 1972: Description of global-scale circulation cells in the tropics
612 with a 40-50 day period. *J. Atmos. Sci.*, **29**, 1109–1123.

613 Moncrieff, M. W., D. E. Waliser, M. J. Miller, M. A. Shapiro, G. R. Asrar, and J. Caughey, 2012:
614 Multiscale convective organization and the YOTC virtual global field campaign. *Bull. Amer.*
615 *Meteor. Soc.*, **93**, 1171–1187.

616 Mori, S., and Coauthors, 2004: Diurnal land-sea rainfall peak migration over Sumatera Island, In-
617 donesian maritime continent, observed by TRMM satellite and intensive rawinsonde soundings.
618 *Mon. Wea. Rev.*, **132**, 2021–2039.

- 619 Oh, J.-H., X. Jiang, D. E. Waliser, M. W. Moncrieff, R. H. Johnson, and P. Ciesielski, 2015: A mo-
620 mentum budget analysis of westerly wind events associated with the Madden–Julian Oscillation
621 during DYNAMO. *J. Atmos. Sci.*, **72**, 3780–3799.
- 622 Qian, J.-H., 2008: Why precipitation is mostly concentrated over islands in the Maritime Conti-
623 nent. *J. Atmos. Sci.*, **65**, 1428–1441.
- 624 Ridout, J., and M. Flatau, 2011: Convectively coupled Kelvin wave propagation past Suma-
625 tra: A June case and corresponding composite analysis. *J. Geophys. Res.*, **116**, doi:10.1029/
626 2010JD014981.
- 627 Rotunno, R., and P. K. Smolarkiewicz, 1991: Further results on lee vortices in low-Froude-number
628 flow. *J. Atmos. Sci.*, **48**, 2204–2211.
- 629 Roundy, P. E., 2008: Analysis of convectively coupled Kelvin waves in the Indian Ocean MJO. *J.*
630 *Atmos. Sci.*, **65**, 1342–1359.
- 631 Schär, C., and D. R. Durran, 1997: Vortex formation and vortex shedding in continuously stratified
632 flows past isolated topography. *J. Atmos. Sci.*, **54**, 534–554.
- 633 Schär, C., and R. B. Smith, 1993a: Shallow-water flow past isolated topography. Part I: Vorticity
634 production and wake formation. *J. Atmos. Sci.*, **50**, 1373–1400.
- 635 Schär, C., and R. B. Smith, 1993b: Shallow-water flow past isolated topography. Part II: Transition
636 to vortex shedding. *J. Atmos. Sci.*, **50**, 1401–1412.
- 637 Schreck, C. J., 2015: Kelvin waves and tropical cyclogenesis: A global survey. *Mon. Wea. Rev.*,
638 **143**, 3996–4011.
- 639 Schreck, C. J., and J. Molinari, 2009: A case study of an outbreak of twin tropical cyclones. *Mon.*
640 *Wea. Rev.*, **137**, 863–875.

- 641 Schreck, C. J., and J. Molinari, 2011: Tropical cyclogenesis associated with Kelvin waves and the
642 Madden-Julian Oscillation. *Mon. Wea. Rev.*, **139**, 2723–2734.
- 643 Serra, Y., G. Kiladis, and K. Hodges, 2010: Tracking and mean structure of easterly waves over
644 the Intra-Americas seas. *J. Climate*, **23**, 4823–4840.
- 645 Smith, R. B., 1989: Hydrostatic flow over mountains. *Advances in Geophysics*, **31**, 1–41.
- 646 Smith, R. B., and Grubišić, 1993: Aerial observations of Hawaii’s wake. *J. Atmos. Sci.*, **50**, 3728–
647 3750.
- 648 Smolarkiewicz, P. K., and R. Rotunno, 1989: Low Froude number flow past three-dimensional
649 obstacles. Part I: Baroclinically generated lee vortices. *J. Atmos. Sci.*, **46**, 1154–1164.
- 650 Waliser, D. E., and Coauthors, 2012: The “Year” of Tropical Convection (May 2008–April 2010):
651 Climate variability and weather highlights. *Bull. Amer. Meteor. Soc.*, **93**, 1189–1218.
- 652 Wheeler, M., and G. N. Kiladis, 1999: Convectively coupled equatorial waves: Analysis of clouds
653 and temperature in the wavenumber-frequency domain. *J. Atmos. Sci.*, **56**, 374–399.
- 654 Wu, C.-H., and H.-H. Hsu, 2009: Topographic influence on the MJO in the Maritime Continent.
655 *J. Climate*, **22**, 5433–5448.
- 656 Wu, P., M. Hara, J.-i. Hamada, M. D. Yamanaka, and F. Kimura, 2009: Why a large amount of rain
657 falls over the sea in the vicinity of western Sumatra Island during nighttime. *J. Appl. Meteor.*
658 *Climatol.*, **48**, 1345–1361.
- 659 Yoneyama, K., C. Zhang, and C. N. Long, 2013: Tracking pulses of the Madden-Julian Oscillation.
660 *Bull. Amer. Meteor. Soc.*, **94**, 1871–1891.

- 661 Zehnder, J. A., D. M. Powell, and D. L. Ropp, 1999: The interaction of easterly waves, orography,
662 and the intertropical convergence zone in the genesis of eastern Pacific tropical cyclones. *Mon.*
663 *Wea. Rev.*, **127**, 1566–1585.
- 664 Zhang, C., 2005: Madden-Julian Oscillation. *Rev. Geophys.*, **89**, RG2003, doi:10.1029/
665 2004RG000158.

666 **LIST OF TABLES**

667 **Table 1.** Vortices (shed and non-shed) and tropical cyclones originating from the four
668 analysis regions in Fig. 2, including totals for easterly ($U_N < 0$ for SN and MP,
669 $U_S < 0$ for SS and JV) and westerly ($U_N > 0$ for SN and MP, $U_S > 0$ for SS and
670 JV) flow regimes. 33

671 **Table 2.** Yearly and summary totals of tropical cyclones (TCs) in the northern and south-
672 ern Indian Ocean (IO) during YOTC and DYNAMO, including numbers and
673 percentages of tropical cyclones originating from terrain-induced vortices. 34

674 **Table 3.** The 13 terrain-induced vortices that developed into named tropical cyclones
675 originating from three analysis regions in Fig. 2 – Sumatra North (SN), Sumatra
676 South (SS), and Java (JV) – during YOTC and DYNAMO. 35

677 TABLE 1. Vortices (shed and non-shed) and tropical cyclones originating from the four analysis regions in
678 Fig. 2, including totals for easterly ($U_N < 0$ for SN and MP, $U_S < 0$ for SS and JV) and westerly ($U_N > 0$ for SN
679 and MP, $U_S > 0$ for SS and JV) flow regimes.

	GENESIS REGION				
	Sumatra	Malay	Sumatra	Java (JV)	Total
	North (SN)	Peninsula (MP)	South (SS)		
Total vortices	73	85	74	77	309
Shed vortices (total)	43	15	25	20	103
Shed vortices (easterly flow)	40	12	18	19	89
Shed vortices (westerly flow)	3	3	7	1	14
Non-shed vortices (total)	30	70	49	57	206
Non-shed vortices (easterly flow)	26	61	36	40	163
Non-shed vortices (westerly flow)	4	9	13	17	43
Tropical cyclones	5	0	6	2	13

680 TABLE 2. Yearly and summary totals of tropical cyclones (TCs) in the northern and southern Indian Ocean
 681 (IO) during YOTC and DYNAMO, including numbers and percentages of tropical cyclones originating from
 682 terrain-induced vortices.

Period	Northern IO	Southern IO	TOTAL
YOTC			
2008 (May – Dec)	7	4	11
2009 (Jan – Dec)	5	12	17
2010 (Jan – Apr)	0	7	7
DYNAMO			
2011 (Oct – Dec)	5	3	8
2012 (Jan – Mar)	0	8	8
TOTAL	17	34	51
Number of TCs from terrain vortices	5	8	13
Percent TCs from terrain vortices	29.4%	23.5%	25.4%

683 TABLE 3. The 13 terrain-induced vortices that developed into named tropical cyclones originating from
684 three analysis regions in Fig. 2 – Sumatra North (SN), Sumatra South (SS), and Java (JV) – during YOTC and
685 DYNAMO.

Storm name	Year	Vortex initiation region	First detection date	TC naming date (JTWC)	Pre-TC duration (days)
Asma	2008	JV	27 Sep	17 Oct	20
03A	2008	SN	08 Oct	21 Oct	13
Nisha	2008	SN	18 Nov	26 Nov	8
07B	2008	SN	29 Nov	04 Dec	5
Gael	2009	SS	15 Jan	03 Feb	19
Cleo	2009	SS	27 Nov	07 Dec	10
Ward	2009	SN	29 Nov	11 Dec	12
David	2009	SS	05 Dec	13 Dec	8
Imani	2010	SS	11 Mar	23 Mar	12
Robyn	2010	SS	26 Mar	02 Apr	7
05A	2011	SN	19 Nov	26 Nov	7
Alenga	2011	JV	30 Nov	05 Dec	5
Benilde	2011	SS	23 Dec	28 Dec	5

686 **LIST OF FIGURES**

687 **Fig. 1.** Analysis domain and topography of the region (elevation scale on right). Delineation of flow
688 regimes is based on zonal wind analyzed along blue lines at 100°E, 3-7°N and 105°E, 3-7°S. 38

689 **Fig. 2.** Cyclonic vortex genesis frequency on a 1° grid for (a) November-April and (b) May-October
690 periods. Streamlines depict 925-850 hPa layer-average flows. Flows in (a) and (b) typify
691 boreal winter and summer monsoon conditions, respectively. 39

692 **Fig. 3.** Monthly frequency of terrain-induced shed (green bars) and non-shed (black bars) cyclonic
693 vortices for (a) Sumatra north (SN) and (b) Malay Peninsula (MP) regions. (c) Monthly
694 mean zonal wind (m s^{-1}) along 100°E (line segment shown in Fig. 1), indicating most
695 cyclonic vortices in these regions occur in mean easterly flow during the boreal winter mon-
696 soon. TC events originating from terrain-induced vortices shown in red. Gray shading
697 indicates period of time with three years of data from both YOTC and DYNAMO; unshaded
698 period has only two years of YOTC data. 40

699 **Fig. 4.** As in Fig. 3, except for (a) Sumatra south (SS) and (b) west Java (JV) regions. (c) Monthly
700 mean zonal wind (m s^{-1}) along 105°E (line segment shown in Fig. 1), indicating cyclonic
701 vortices in these regions can occur during both easterly and westerly mean flow. TC events
702 originating from terrain-induced vortices shown in red. 41

703 **Fig. 5.** Tracks for all cyclonic vortices lasting longer than two days originating between 10°N and
704 10°S, 50°-110°E determined by the objective tracking scheme. Prominent origination sites
705 can be seen near Sumatra, the Malay Peninsula, west Java, southern India, and Sri Lanka. 42

706 **Fig. 6.** As in Fig. 5, except only for cyclonic vortices emanating from the four analysis regions:
707 Sumatra north (SN, red), Malay Peninsula (MP, blue), Sumatra south (SS, green), and west
708 Java (JV, purple). 43

709 **Fig. 7.** Mean 925-850 hPa flow over Indian Ocean basin for (a) shed (40 cases) and (b) non-shed
710 (26 cases) cyclonic vortices from region SN (black box shown) under conditions of easterly
711 flow across northern Sumatra. 44

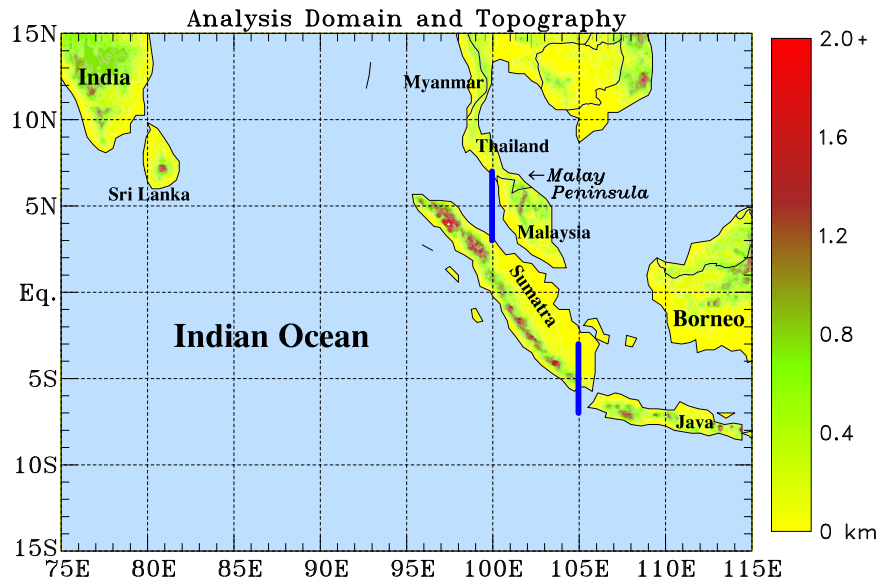
712 **Fig. 8.** Mean 925-850 hPa flow over Indian Ocean basin for shed vortices from region SS (black
713 box shown) under conditions of (a) easterly (18 cases) and (b) westerly (7 cases) flow in the
714 analysis region. 45

715 **Fig. 9.** Mean 925-850 hPa average streamlines and relative vorticity (scale at bottom) during DY-
716 NAMO (October 2011 to March 2012) for all (a) easterly and (b) westerly wind days, as
717 determined by the zonal wind incident upon northern Sumatra. Fields shown are means
718 for days when $|U_N| > 5 \text{ m s}^{-1}$. Panels (a) and (b) include 97 and 23 six-hourly analyses,
719 respectively. 46

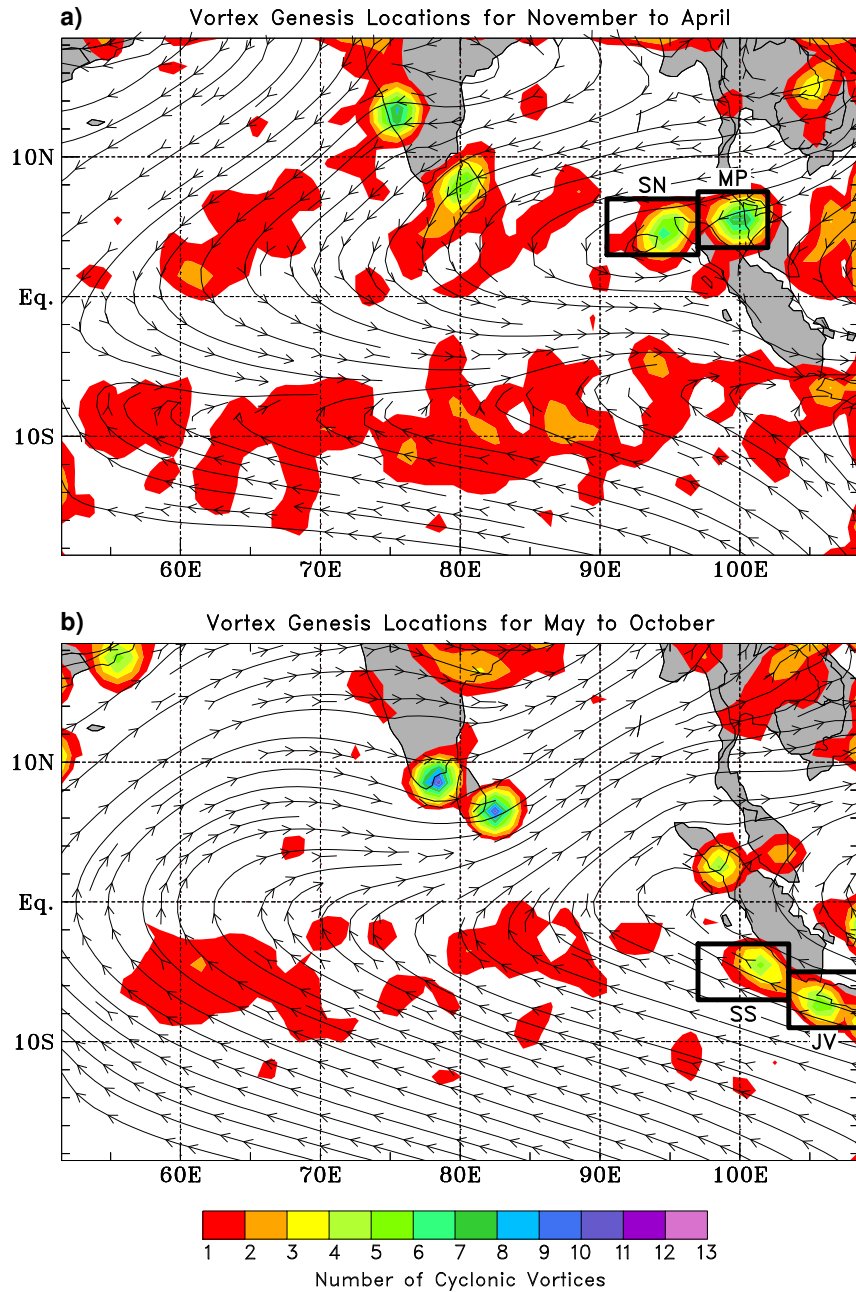
720 **Fig. 10.** Correlations between relative vorticity and zonal wind speeds U_N and U_S along northern
721 and southern line segments, respectively, in Fig. 1 during the 2.5 years of YOTC and DY-
722 NAMO for regions SN, MP, SS, and JV. The magnitudes of the correlations maximize in the
723 lower troposphere (between 925 and 850 hPa in the north and near the surface in the south),
724 indicating the key role of topography in generating the low-level circulations. 47

725 **Fig. 11.** Relative vorticity regressed onto average zonal wind speeds U_N and U_S at 900 hPa along
726 northern and southern line segments, respectively, in Fig. 1 during for 2.5 years of YOTC
727 and DYNAMO for regions SN, MP, SS, and JV. Each data point consists of a concurrent

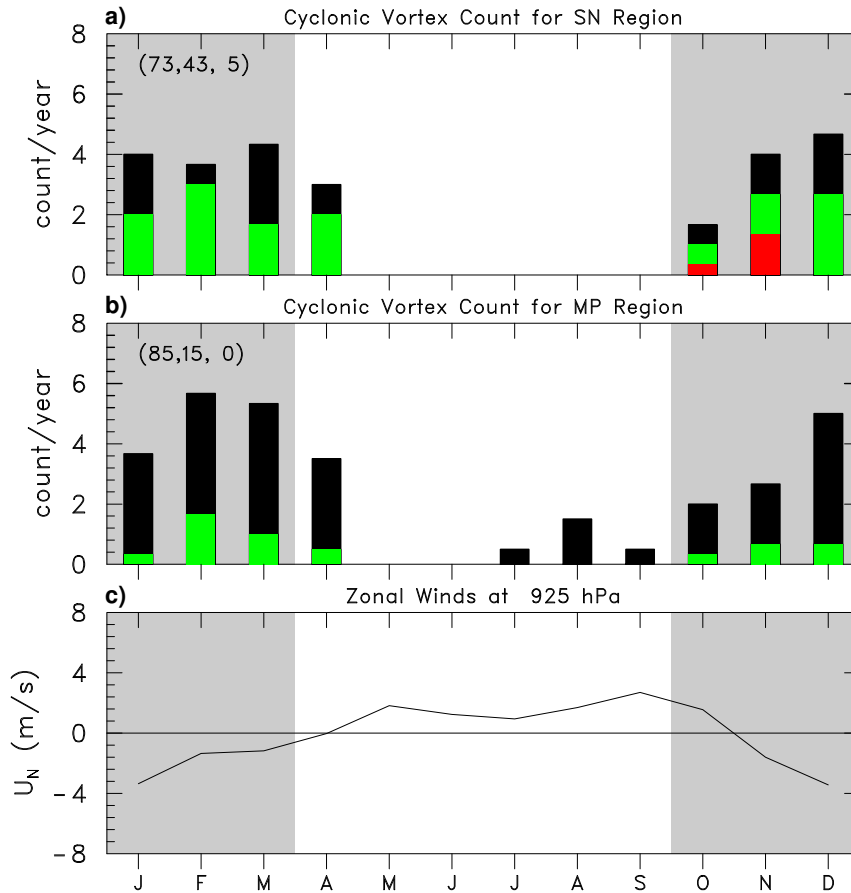
728	daily-averaged relative vorticity and zonal wind value. Solid lines are linear least-squares	
729	best fits to the data. Correlation coefficients r are indicated.	48
730	Fig. 12. Time-longitude diagrams of daily-averaged 850-hPa relative vorticity (color, scale at bot-	
731	tom) and zonal wind (contours) for OND2008 at (a) 850 hPa, averaged over 3-7°N, and	
732	(b) 925 hPa, averaged over 3-7°S. Zonal wind contour spacing: 0, 2.5, and 5 m s ⁻¹ . Solid	
733	(dashed) thick black contours indicate westerly (easterly) winds, and the solid thin black	
734	contour denotes zero wind. Longitudes and days when wake vortices reached tropical storm	
735	strength marked by tropical storm symbols. Sumatra's central longitude marked by black	
736	dashed vertical line at 100°E. TCs may move out of the latitude averaging bands, which	
737	may account for apparent discrepancies between the "end" of a vorticity streamer and the	
738	location of tropical cyclogenesis.	49
739	Fig. 13. As in Fig. 12, for OND2009.	50
740	Fig. 14. As in Fig. 12, for OND2011.	51
741	Fig. 15. Tracks of Indian Ocean tropical cyclones that originated from Sumatra-region terrain-	
742	induced vortices during (a) May 2008–April 2009, (b) May 2009–April 2010, and (c) Octo-	
743	ber 2011–March 2012 tropical cyclone seasons. Thin lines represent tracks of wake vortices	
744	before they developed into named TCs. Thick lines denote tracks of named TCs.	52
745	Fig. 16. 850-hPa scaled wind vectors and geopotential height anomalies (scales at bottom) for (a)	
746	29 Nov, (b) 30 Nov, (c) 1 Dec, (d) 2 Dec, (e) 3 Dec, and (f) 4 Dec 2008, showing in (a)-	
747	(d) the wake vortex precursor to TC 07B. TC 07B was officially named a storm on 4 Dec.	
748	Geopotential height anomalies were calculated as the difference from a 10°S to 10°N, Indian	
749	Ocean-wide (35-120°E) geopotential height mean during OND of the same year.	53
750	Fig. 17. As in Fig. 16, except for (a) 2 Dec, (b) 3 Dec, (c) 4 Dec, (d) 5 Dec, (e) 6 Dec, and (f) 7	
751	Dec 2009, showing the wake vortex precursors to TCs Cleo (labeled "C"), Ward ("W"), and	
752	David ("D"). TCs Cleo, Ward, and David were officially named storms on 7, 11, and 13	
753	Dec, respectively.	54
754	Fig. 18. As in Fig. 16, except for (a) 19 Nov, (b) 20 Nov, (c) 21 Nov, (d) 22 Nov, (e) 23 Nov, and	
755	(f) 24 Nov 2011, showing the wake vortex precursor to TC 05A. TC 05A was an officially	
756	named storm on 26 Nov. Dark green contour is -10 W m^{-2} MJO-filtered OLR anomaly,	
757	indicating eastward progression of the MJO.	55
758	Fig. 19. Time-longitude diagrams of daily-averaged relative vorticity (color, scale at bottom) and	
759	contours representing OLR anomalies filtered by (a) equatorial Rossby waves and (b) Kelvin	
760	waves for OND2011. Solid contours represent OLR anomalies of 5 and 15 W m^{-2} , and	
761	dashed contours represent OLR anomalies of -5 and -15 W m^{-2} , indicating increased cloudi-	
762	ness.	56



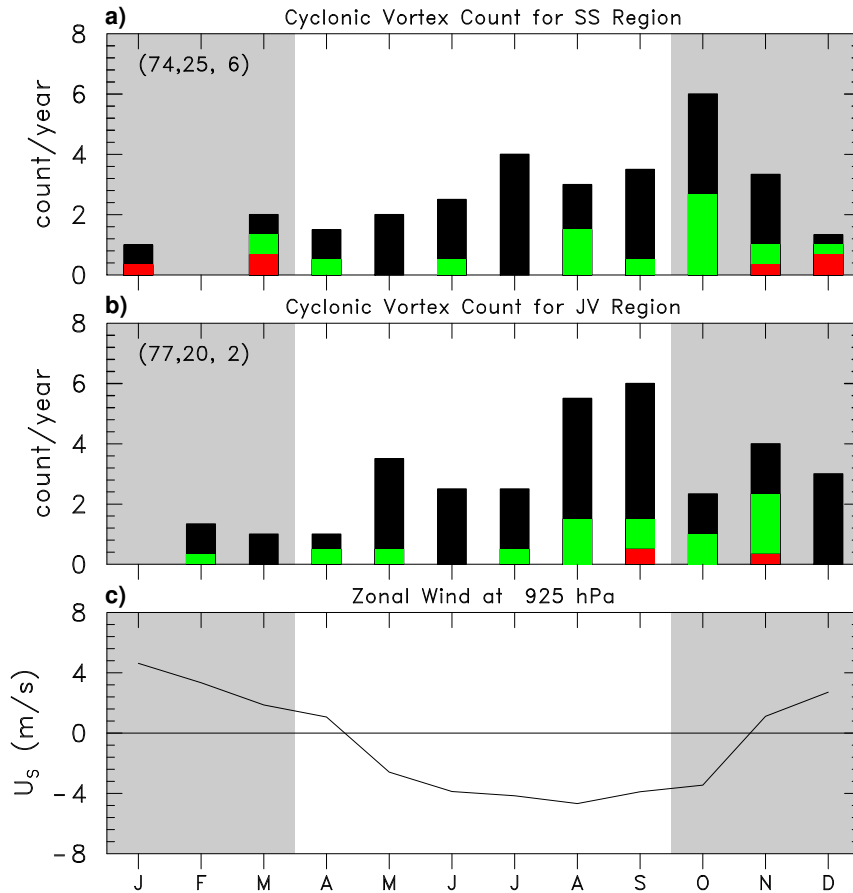
763 FIG. 1. Analysis domain and topography of the region (elevation scale on right). Delineation of flow regimes
 764 is based on zonal wind analyzed along blue lines at 100°E, 3-7°N and 105°E, 3-7°S.



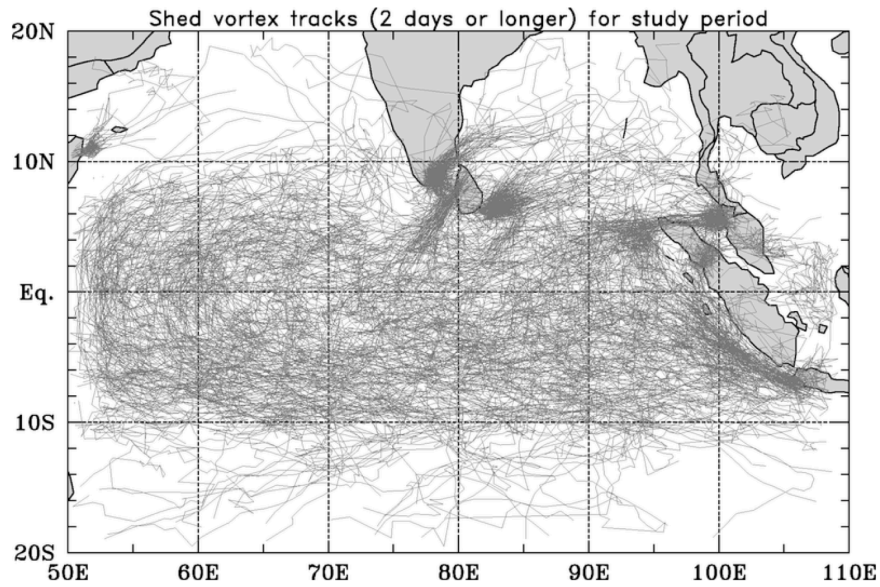
765 FIG. 2. Cyclonic vortex genesis frequency on a 1° grid for (a) November-April and (b) May-October periods.
 766 Streamlines depict 925-850 hPa layer-average flows. Flows in (a) and (b) typify boreal winter and summer
 767 monsoon conditions, respectively.



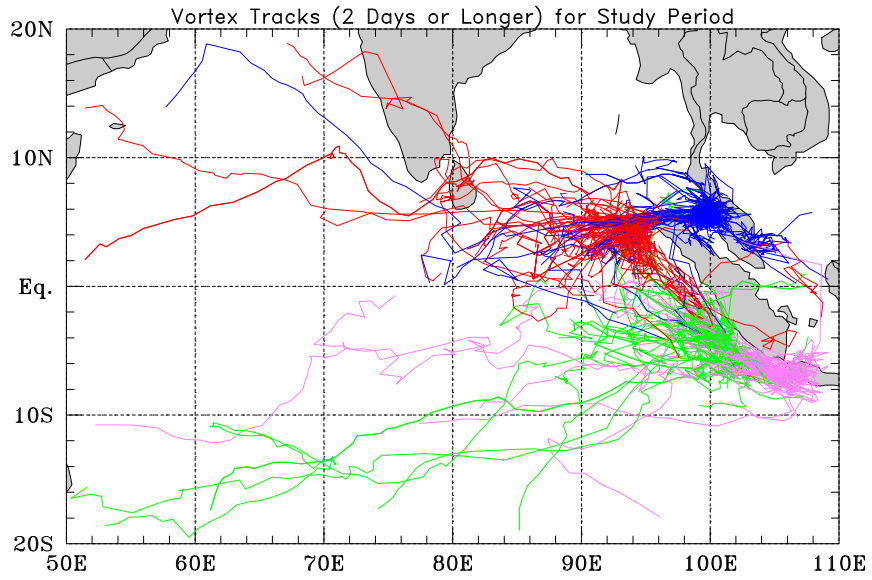
768 FIG. 3. Monthly frequency of terrain-induced shed (green bars) and non-shed (black bars) cyclonic vortices
 769 for (a) Sumatra north (SN) and (b) Malay Peninsula (MP) regions. (c) Monthly mean zonal wind (m s^{-1}) along
 770 100°E (line segment shown in Fig. 1), indicating most cyclonic vortices in these regions occur in mean easterly
 771 flow during the boreal winter monsoon. TC events originating from terrain-induced vortices shown in red. Gray
 772 shading indicates period of time with three years of data from both YOTC and DYNAMO; unshaded period has
 773 only two years of YOTC data.



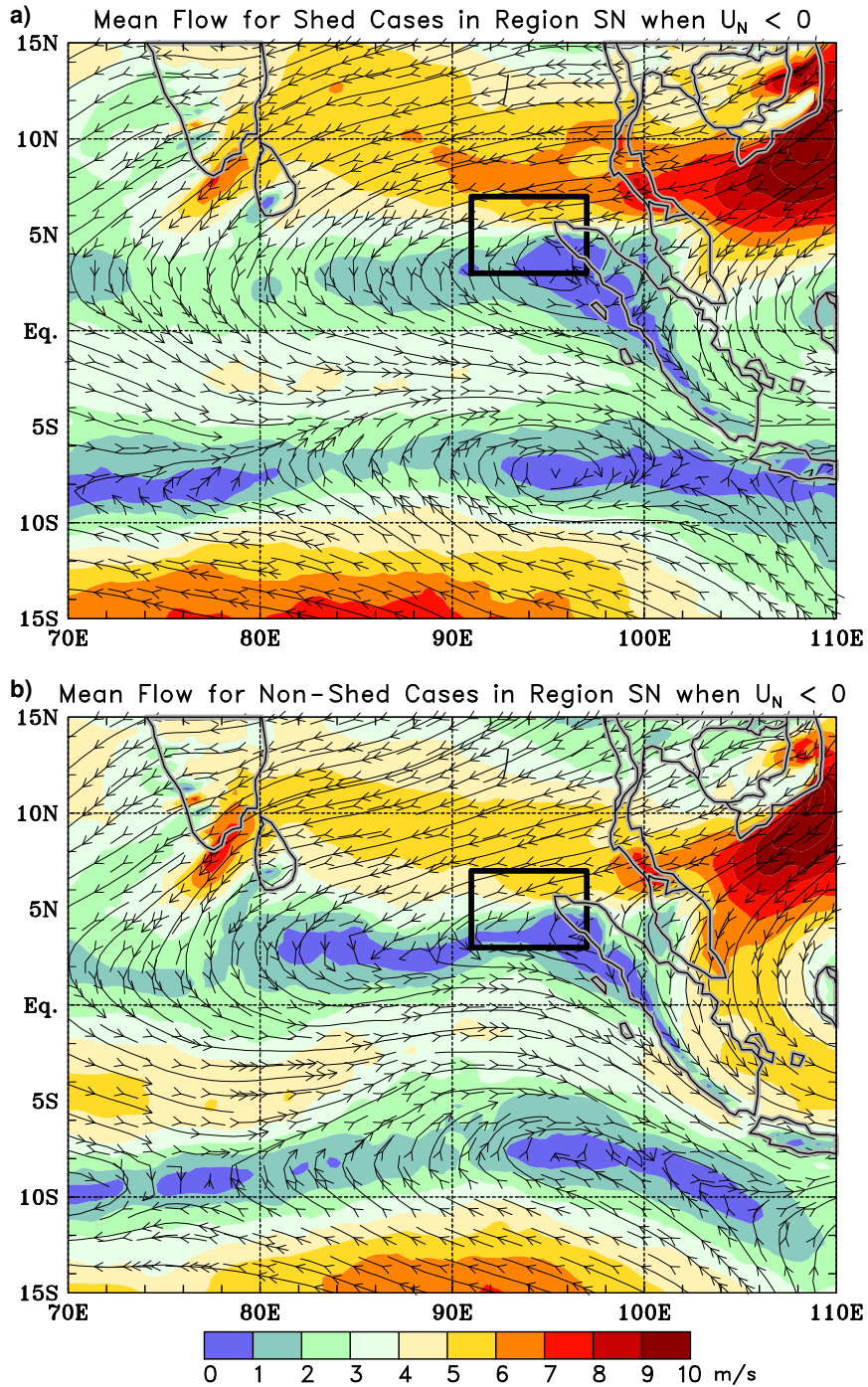
774 FIG. 4. As in Fig. 3, except for (a) Sumatra south (SS) and (b) west Java (JV) regions. (c) Monthly mean
 775 zonal wind (m s^{-1}) along 105°E (line segment shown in Fig. 1), indicating cyclonic vortices in these regions can
 776 occur during both easterly and westerly mean flow. TC events originating from terrain-induced vortices shown
 777 in red.



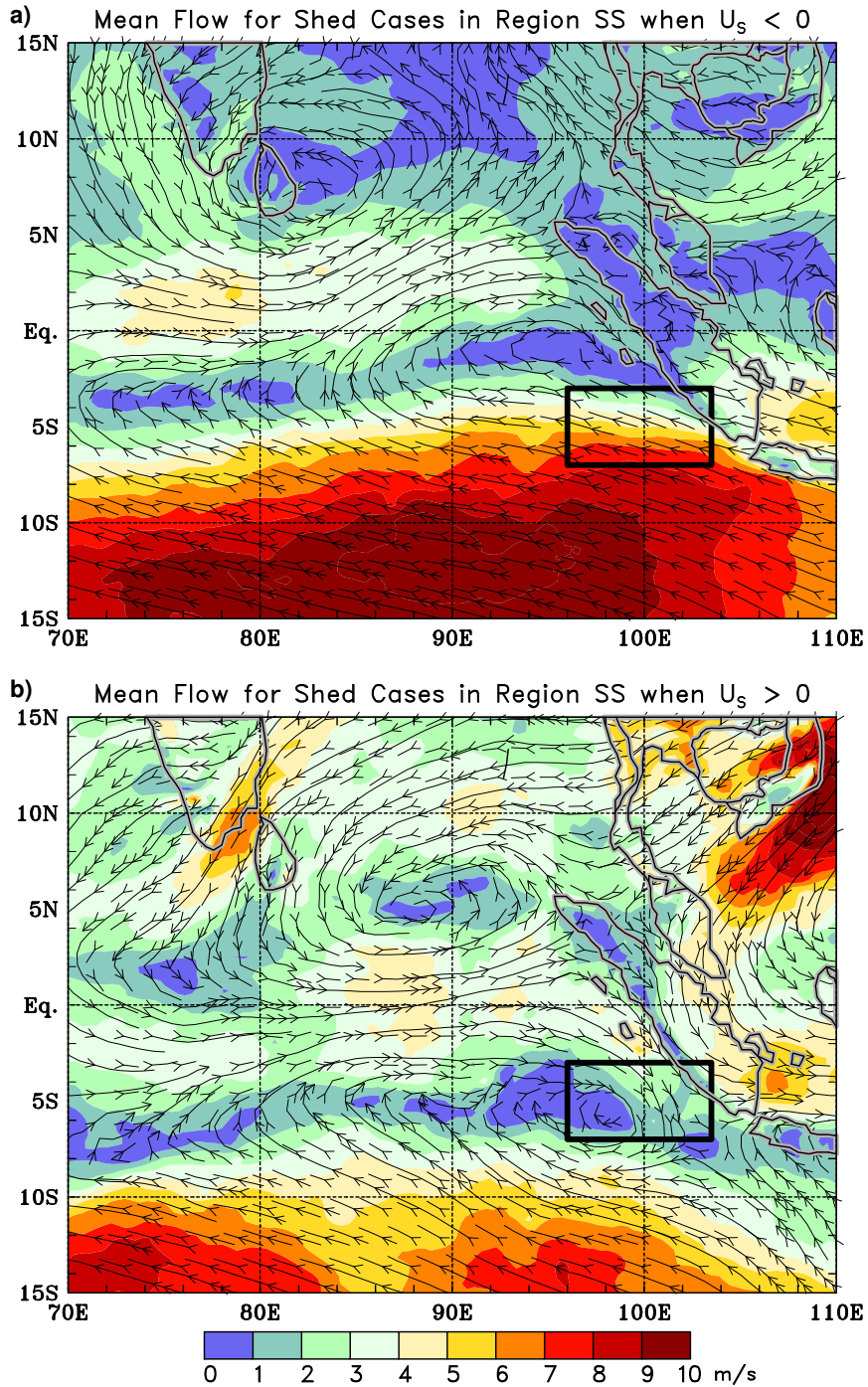
778 FIG. 5. Tracks for all cyclonic vortices lasting longer than two days originating between 10°N and 10°S,
779 50°-110°E determined by the objective tracking scheme. Prominent origination sites can be seen near Sumatra,
780 the Malay Peninsula, west Java, southern India, and Sri Lanka.



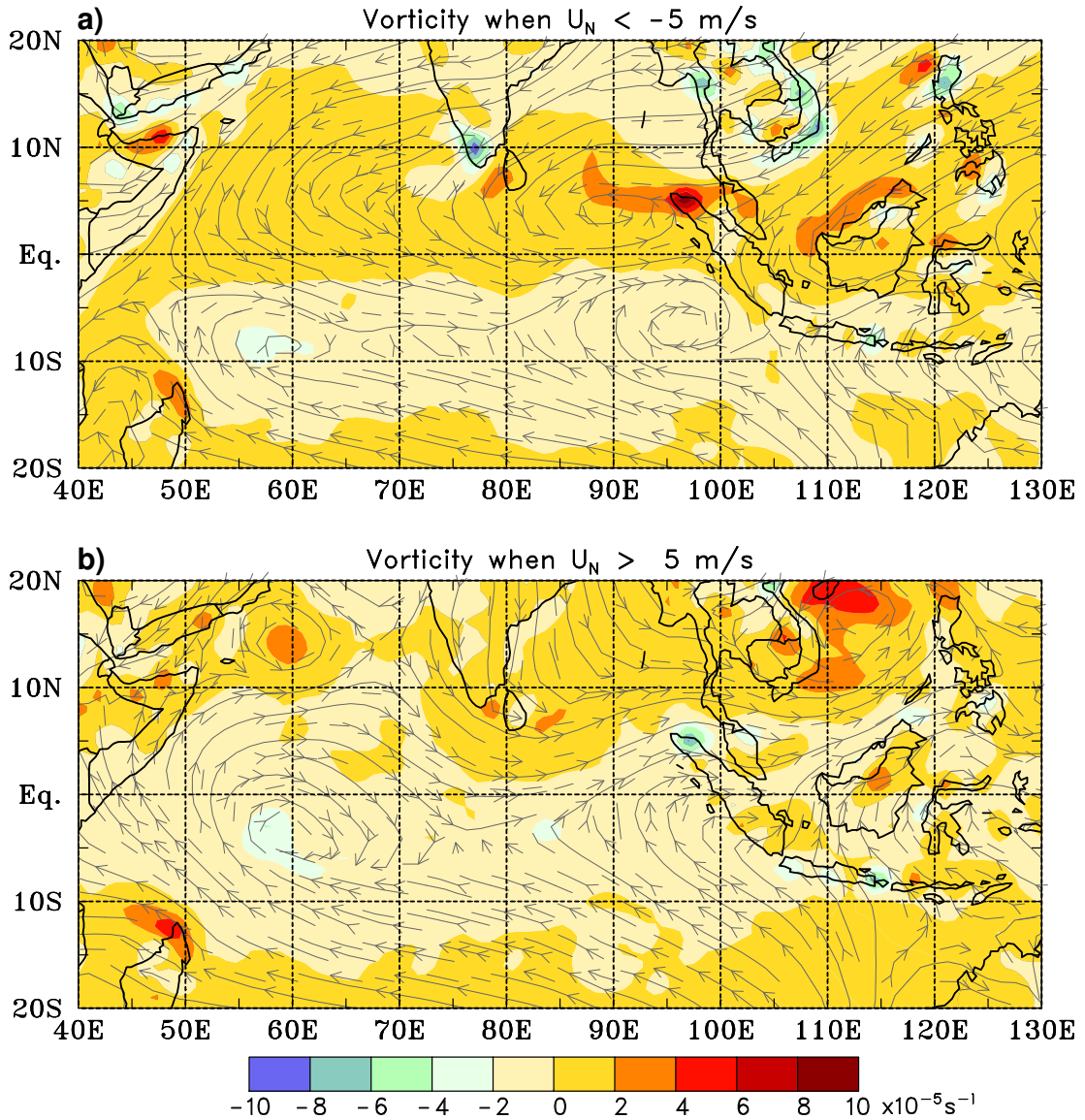
781 FIG. 6. As in Fig. 5, except only for cyclonic vortices emanating from the four analysis regions: Sumatra
782 north (SN, red), Malay Peninsula (MP, blue), Sumatra south (SS, green), and west Java (JV, purple).



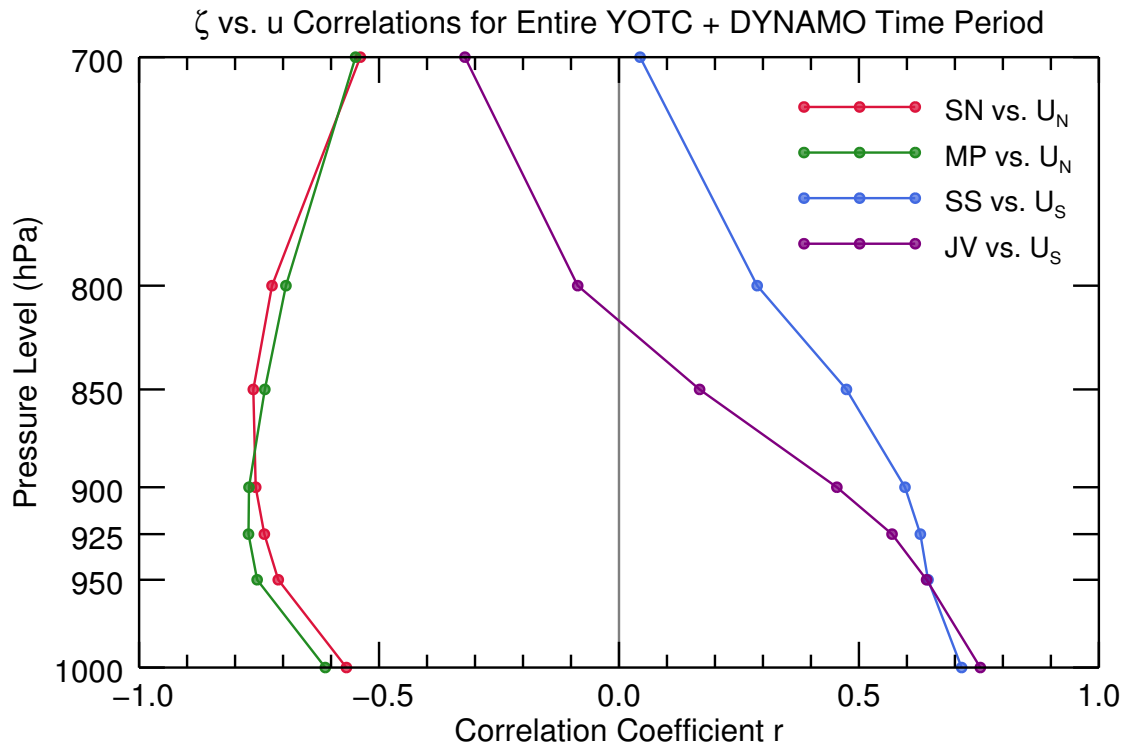
783 FIG. 7. Mean 925-850 hPa flow over Indian Ocean basin for (a) shed (40 cases) and (b) non-shed (26 cases)
 784 cyclonic vortices from region SN (black box shown) under conditions of easterly flow across northern Sumatra.



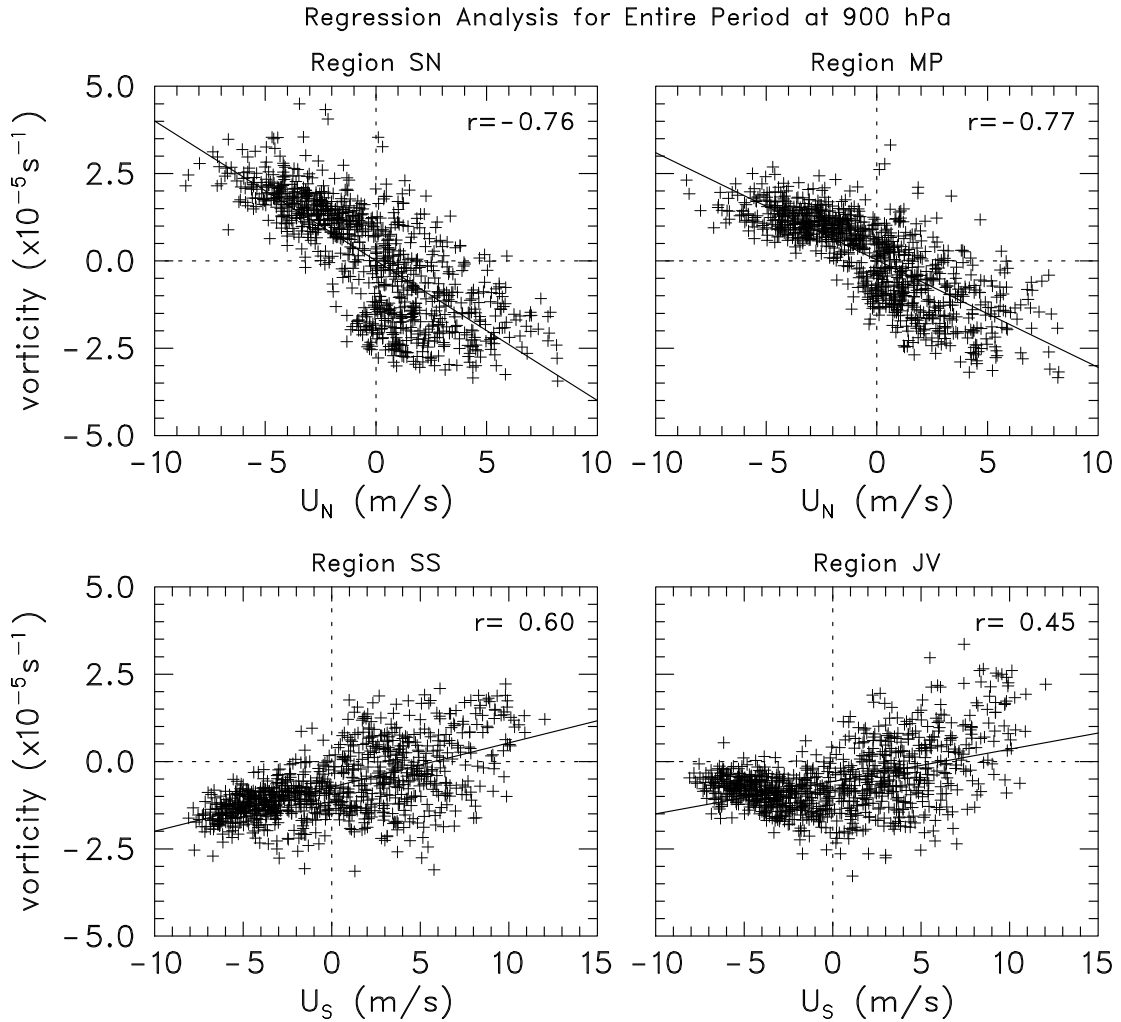
785 FIG. 8. Mean 925-850 hPa flow over Indian Ocean basin for shed vortices from region SS (black box shown)
 786 under conditions of (a) easterly (18 cases) and (b) westerly (7 cases) flow in the analysis region.



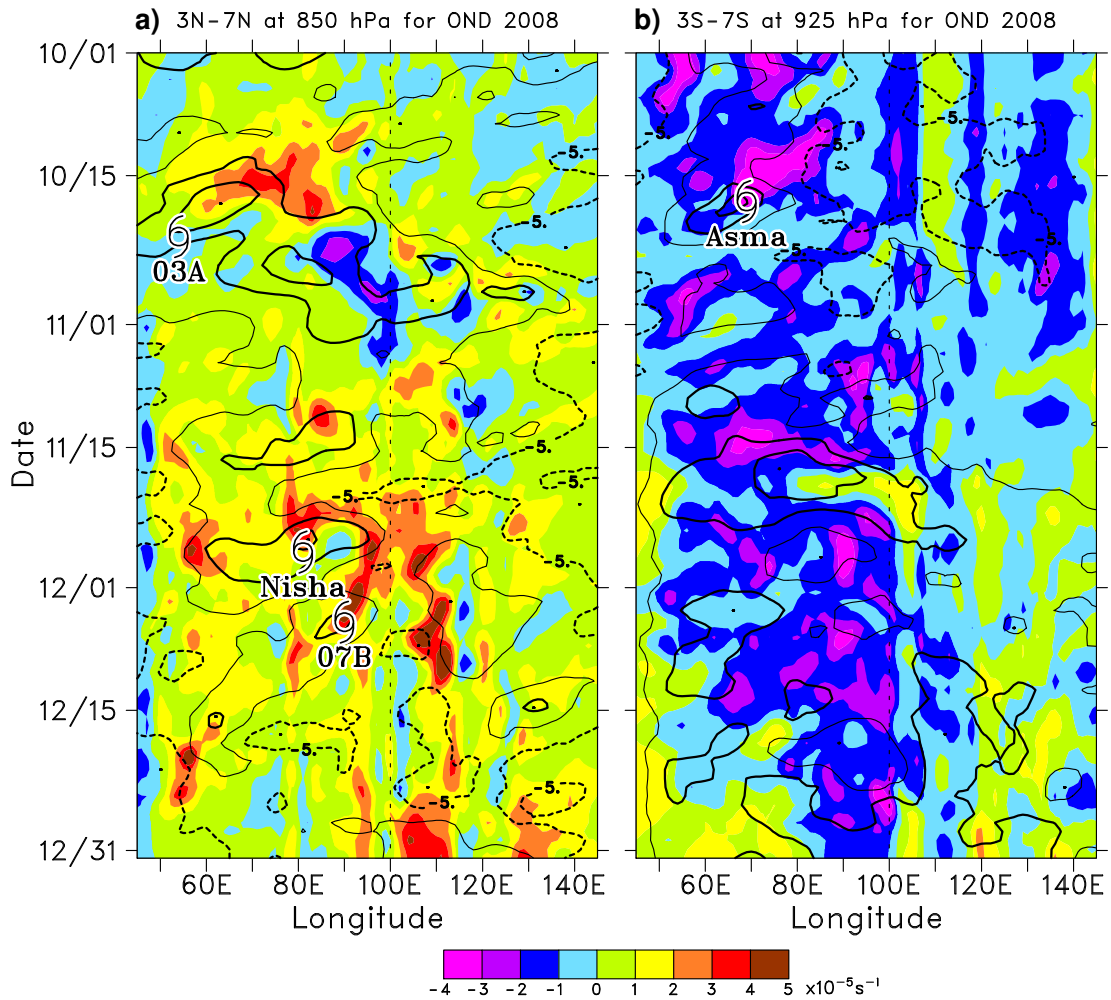
787 FIG. 9. Mean 925-850 hPa average streamlines and relative vorticity (scale at bottom) during DYNAMO
 788 (October 2011 to March 2012) for all (a) easterly and (b) westerly wind days, as determined by the zonal wind
 789 incident upon northern Sumatra. Fields shown are means for days when $|U_N| > 5 \text{ m s}^{-1}$. Panels (a) and (b)
 790 include 97 and 23 six-hourly analyses, respectively.



791 FIG. 10. Correlations between relative vorticity and zonal wind speeds U_N and U_S along northern and southern
 792 line segments, respectively, in Fig. 1 during the 2.5 years of YOTC and DYNAMO for regions SN, MP, SS, and
 793 JV. The magnitudes of the correlations maximize in the lower troposphere (between 925 and 850 hPa in the north
 794 and near the surface in the south), indicating the key role of topography in generating the low-level circulations.



795 FIG. 11. Relative vorticity regressed onto average zonal wind speeds U_N and U_S at 900 hPa along northern
 796 and southern line segments, respectively, in Fig. 1 during for 2.5 years of YOTC and DYNAMO for regions SN,
 797 MP, SS, and JV. Each data point consists of a concurrent daily-averaged relative vorticity and zonal wind value.
 798 Solid lines are linear least-squares best fits to the data. Correlation coefficients r are indicated.



799 FIG. 12. Time-longitude diagrams of daily-averaged 850-hPa relative vorticity (color, scale at bottom) and
800 zonal wind (contours) for OND2008 at (a) 850 hPa, averaged over 3-7°N, and (b) 925 hPa, averaged over 3-7°S.
801 Zonal wind contour spacing: 0, 2.5, and 5 m s^{-1} . Solid (dashed) thick black contours indicate westerly (easterly)
802 winds, and the solid thin black contour denotes zero wind. Longitudes and days when wake vortices reached
803 tropical storm strength marked by tropical storm symbols. Sumatra's central longitude marked by black dashed
804 vertical line at 100°E. TCs may move out of the latitude averaging bands, which may account for apparent
805 discrepancies between the “end” of a vorticity streamer and the location of tropical cyclogenesis.

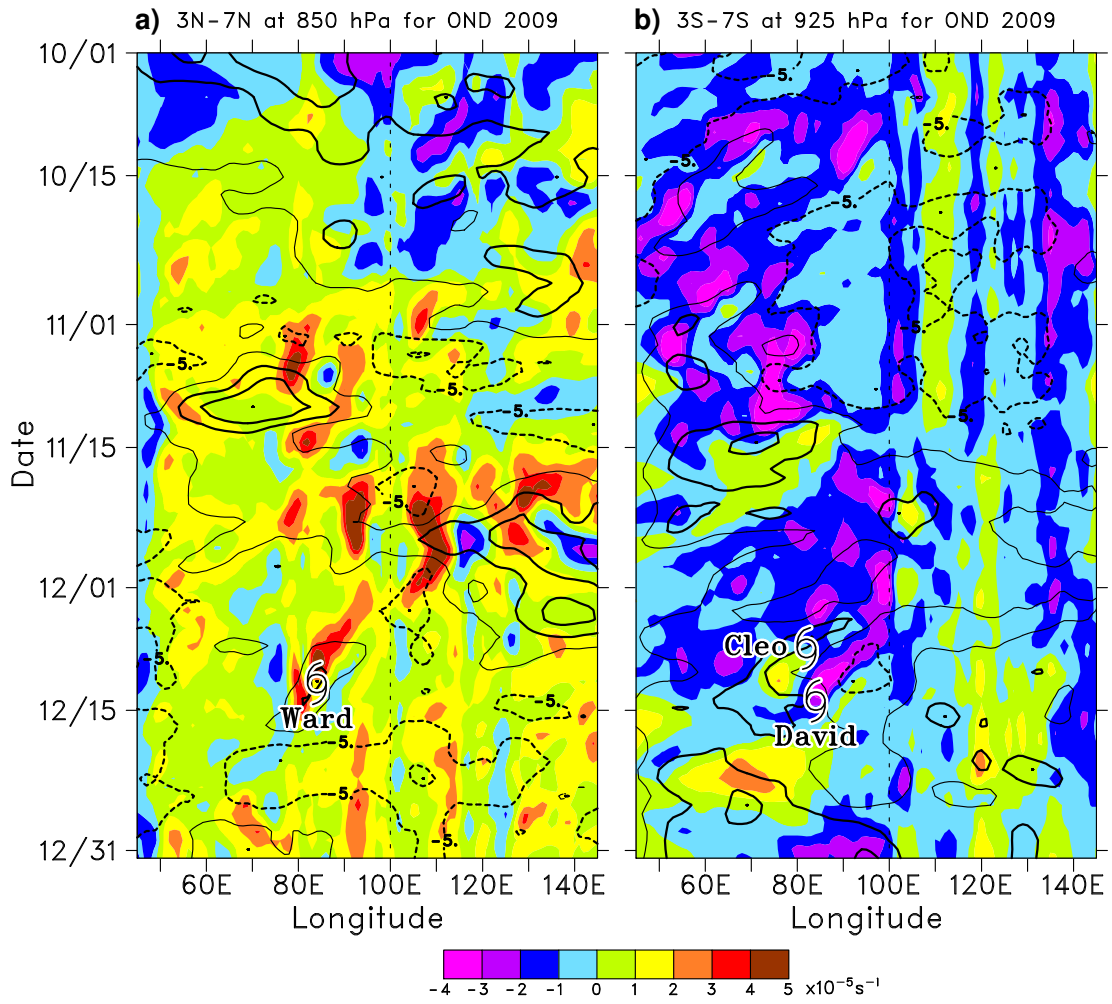


FIG. 13. As in Fig. 12, for OND2009.

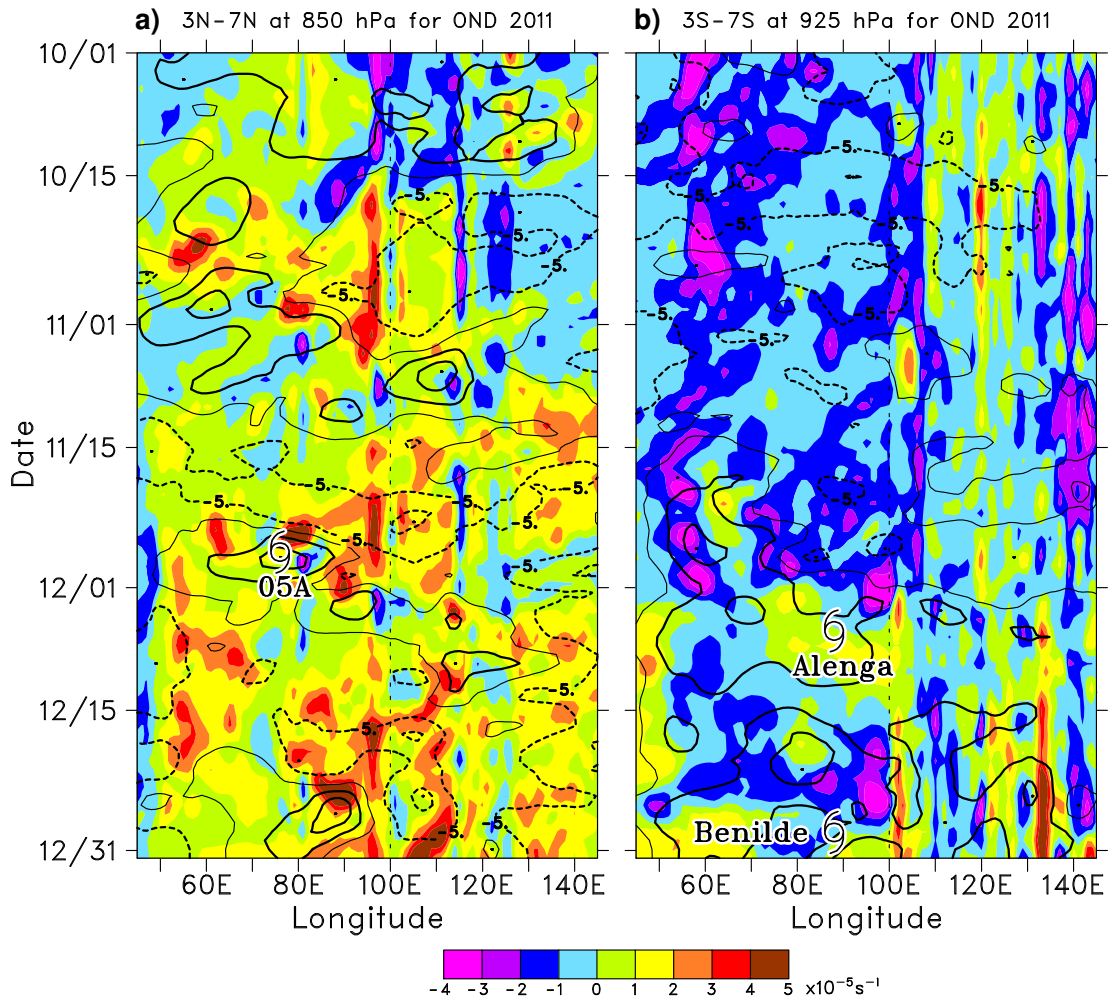
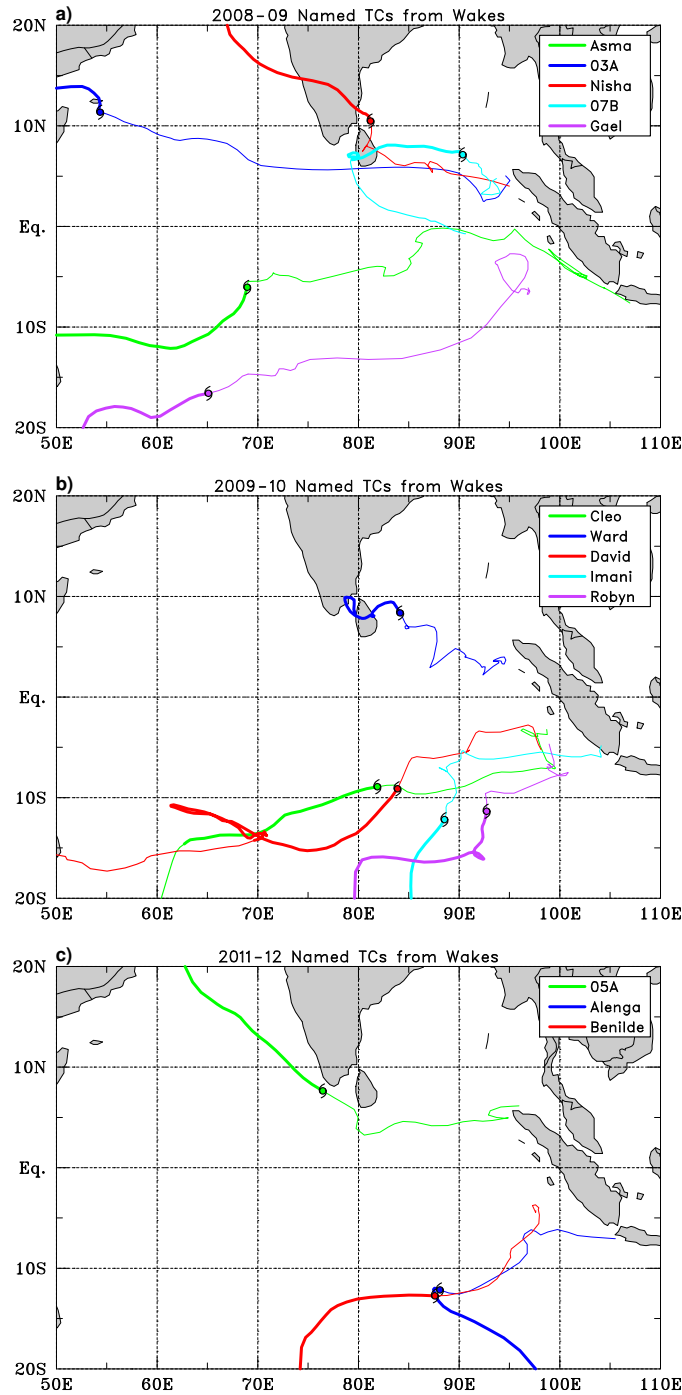
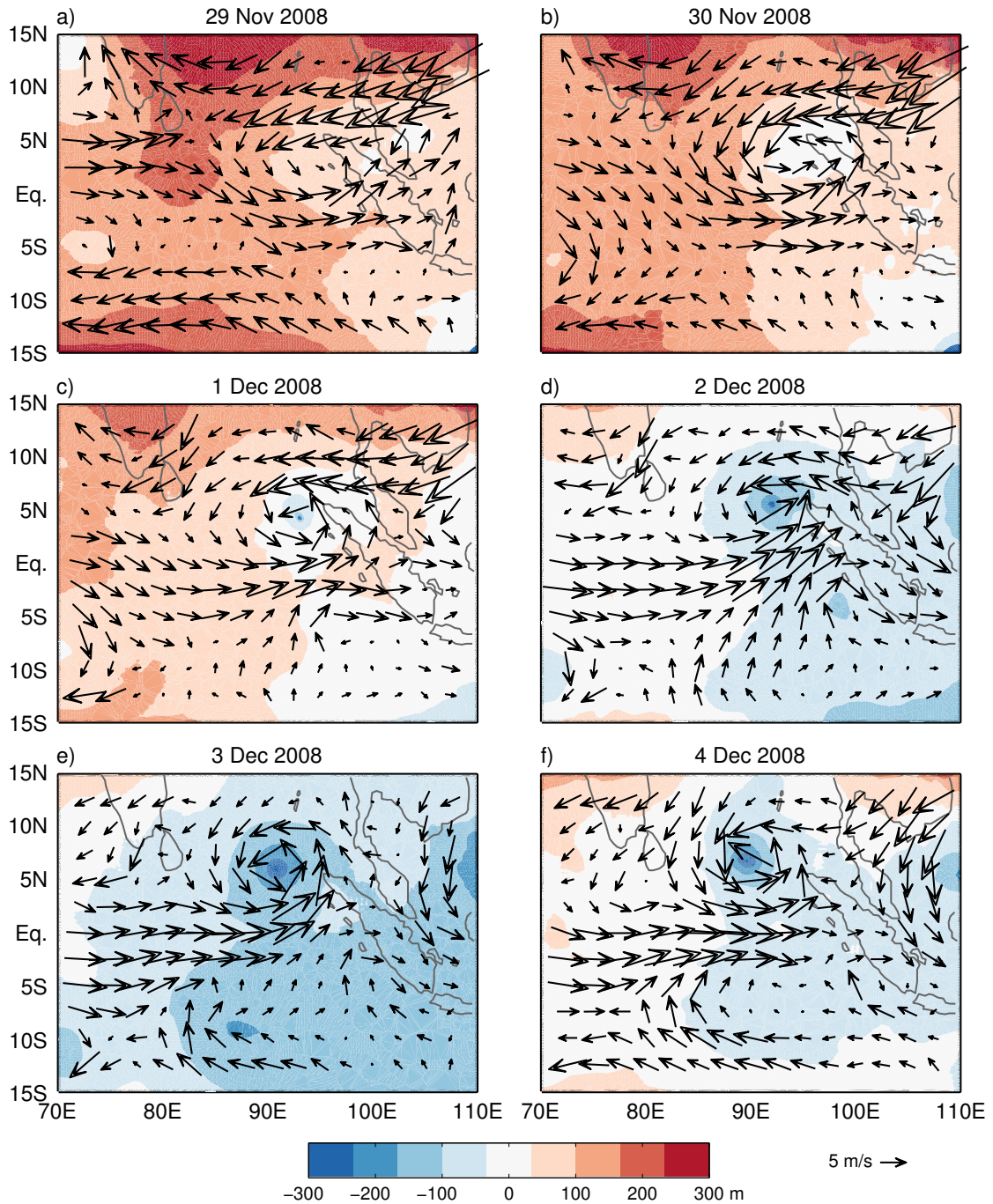


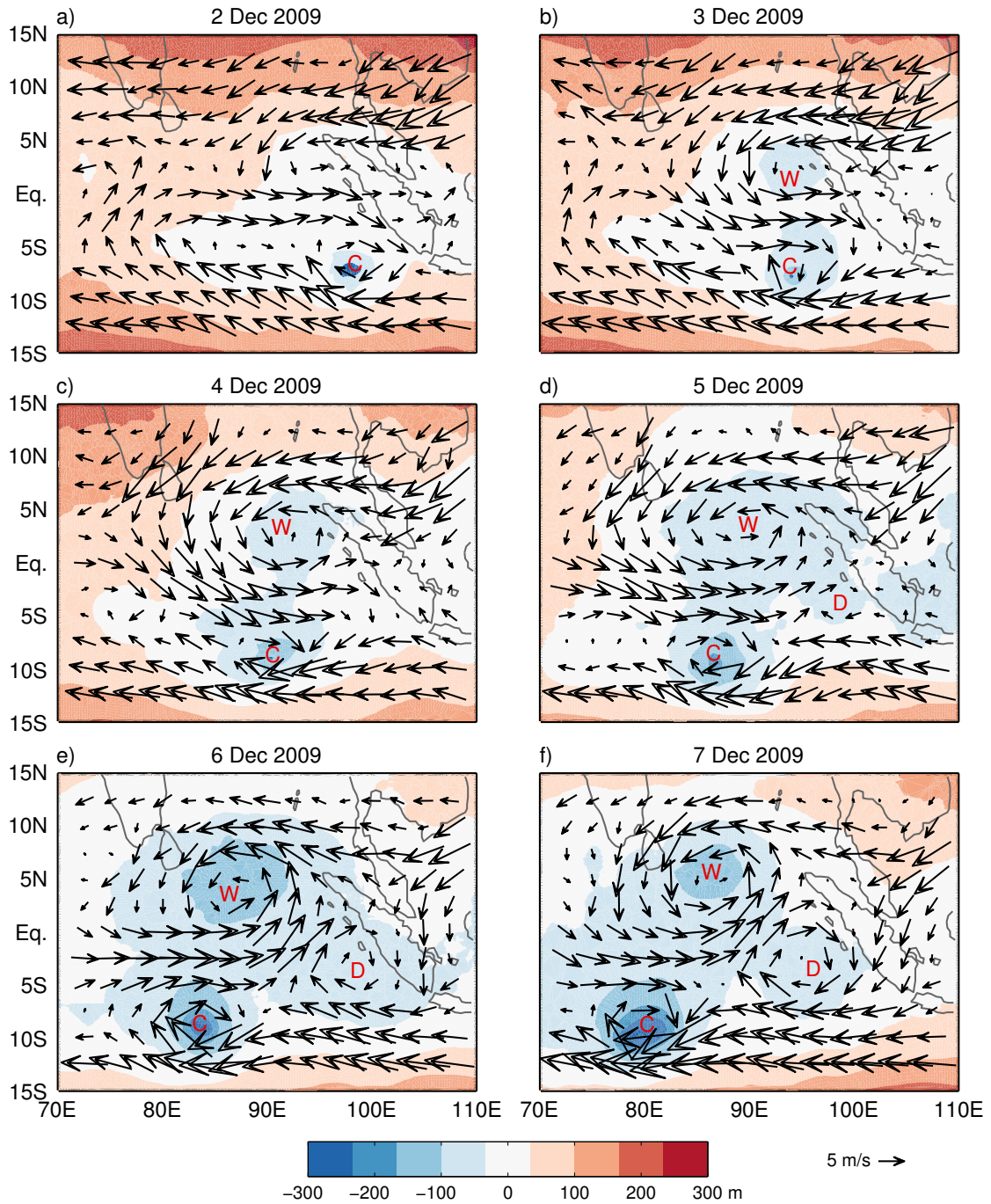
FIG. 14. As in Fig. 12, for OND2011.



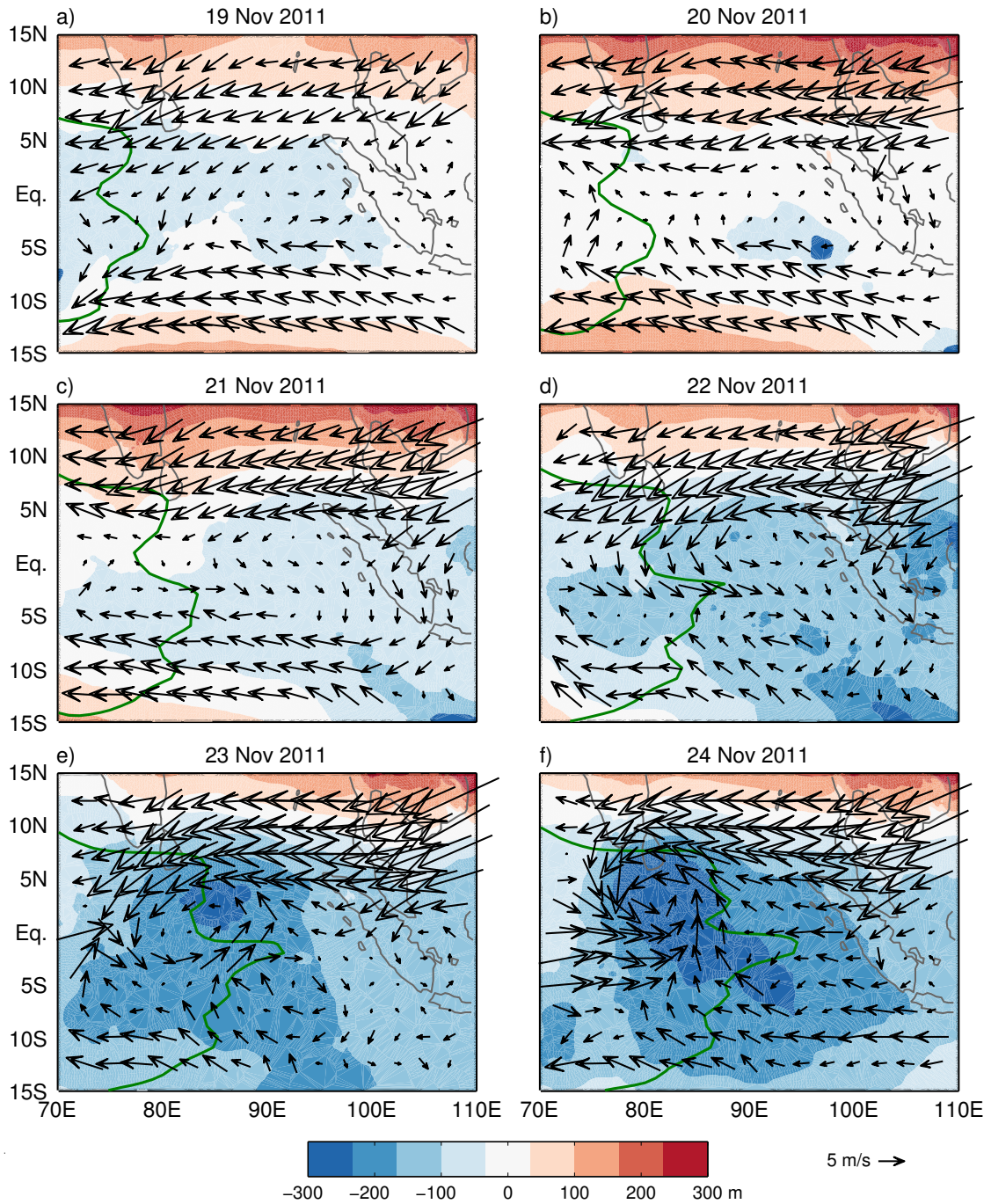
806 FIG. 15. Tracks of Indian Ocean tropical cyclones that originated from Sumatra-region terrain-induced vor-
 807 tices during (a) May 2008–April 2009, (b) May 2009–April 2010, and (c) October 2011–March 2012 tropical
 808 cyclone seasons. Thin lines represent tracks of wake vortices before they developed into named TCs. Thick
 809 lines denote tracks of named TCs.



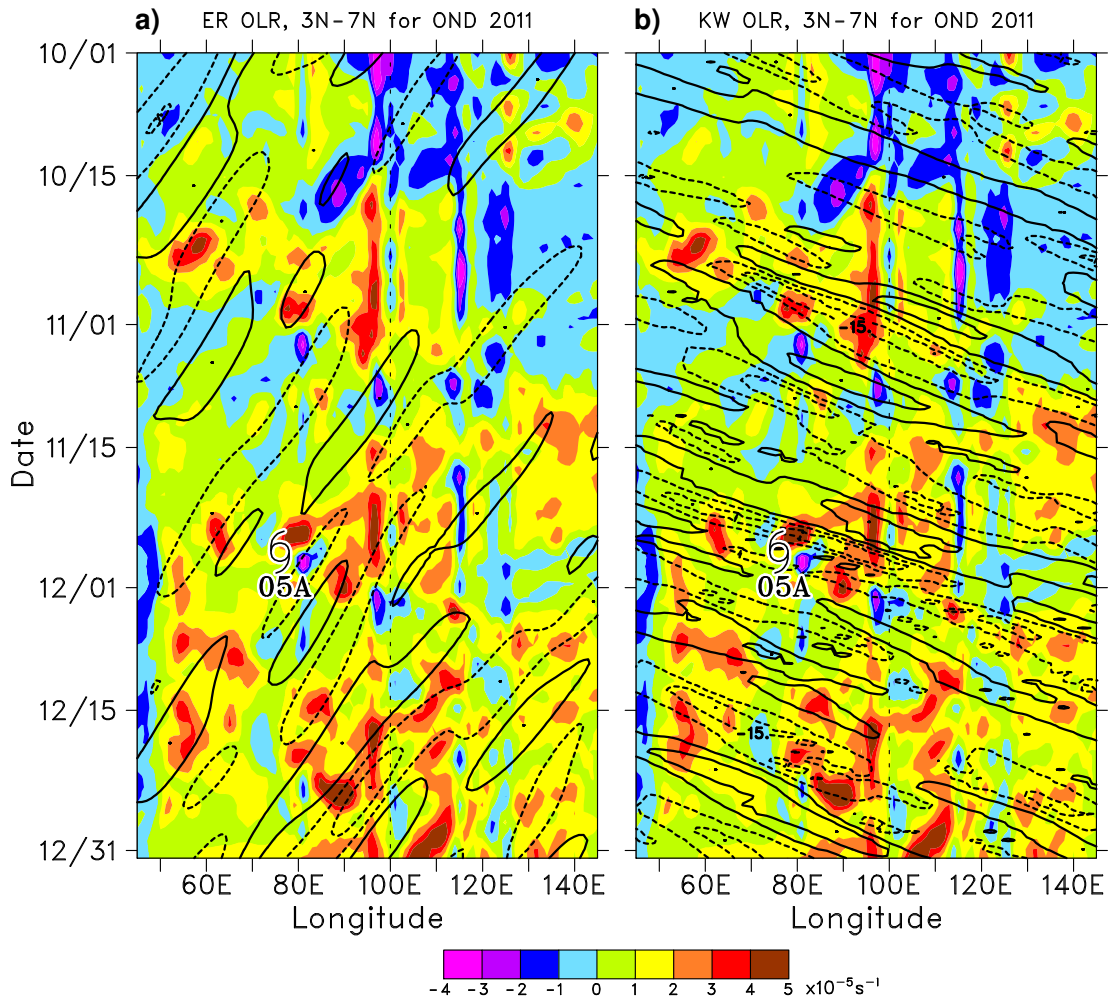
810 FIG. 16. 850-hPa scaled wind vectors and geopotential height anomalies (scales at bottom) for (a) 29 Nov,
 811 (b) 30 Nov, (c) 1 Dec, (d) 2 Dec, (e) 3 Dec, and (f) 4 Dec 2008, showing in (a)-(d) the wake vortex precursor to
 812 TC 07B. TC 07B was officially named a storm on 4 Dec. Geopotential height anomalies were calculated as the
 813 difference from a 10°S to 10°N, Indian Ocean-wide (35-120°E) geopotential height mean during OND of the
 814 same year.



815 FIG. 17. As in Fig. 16, except for (a) 2 Dec, (b) 3 Dec, (c) 4 Dec, (d) 5 Dec, (e) 6 Dec, and (f) 7 Dec 2009,
 816 showing the wake vortex precursors to TCs Cleo (labeled “C”), Ward (“W”), and David (“D”). TCs Cleo, Ward,
 817 and David were officially named storms on 7, 11, and 13 Dec, respectively.



818 FIG. 18. As in Fig. 16, except for (a) 19 Nov, (b) 20 Nov, (c) 21 Nov, (d) 22 Nov, (e) 23 Nov, and (f) 24 Nov
 819 2011, showing the wake vortex precursor to TC 05A. TC 05A was an officially named storm on 26 Nov. Dark
 820 green contour is -10 W m^{-2} MJO-filtered OLR anomaly, indicating eastward progression of the MJO.



821 FIG. 19. Time-longitude diagrams of daily-averaged relative vorticity (color, scale at bottom) and contours
 822 representing OLR anomalies filtered by (a) equatorial Rossby waves and (b) Kelvin waves for OND2011. Solid
 823 contours represent OLR anomalies of 5 and 15 W m^{-2} , and dashed contours represent OLR anomalies of -5 and
 824 -15 W m^{-2} , indicating increased cloudiness.